# Magnetic Super-Exchange with Ultra Cold Atoms in Spin Dependent Optical Lattices

by

David Hucul

Submitted to the Department of Physics
in partial fulfillment of the requirements for the degree of

Master of Science in Physics

at the

MASSACHUSETTS INSTITUTE OF TECHNOLOGY

June 2009



Author .....
Department of Physics
May 22, 2009

Certified by ..... .....
Wolfgang Ketterle
John D. MacArthur Professor of Physics
Thesis Supervisor

Certified by ..... .....
David Pritchard
Cecil and Ida Green Professor of Physics
Thesis Supervisor

Accepted by ... ...
Thomas Greytak
Associate Department Head for Education

# Magnetic Super-Exchange with Ultra Cold Atoms in Spin Dependent Optical Lattices

by

David Hucul

Submitted to the Department of Physics
on May 22, 2009, in partial fulfillment of the
requirements for the degree of
Master of Science in Physics

## Abstract

The methods of atomic physics offer a unique opportunity to study strongly correlated many body systems. It is possible to confine BECs in periodic optical lattices to form an analog of a solid state system. The study of these cold atoms in optical lattice systems may prove a very useful testing ground for novel states of matter, testing fundamental condensed matter theory, and may help illuminate a possible connection between the mechanism behind high temperature superconductivity and quantum magnetism.

This thesis will focus on trapping cold bosonic atoms in spin dependent optical lattices to engineer a system that behaves according to the Hubbard model. By loading the atoms into a state dependent lattice, it may be possible to explore the full phase space of the Heisenberg model and see magnetic super exchange-driven magnetic ordering in a variety of lattice geometries. The aim of this thesis is primarily to explore some of the tools that may be needed accomplish this task.

Thesis Supervisor: Wolfgang Ketterle
Title: John D. MacArthur Professor of Physics

Thesis Supervisor: David Pritchard
Title: Cecil and Ida Green Professor of Physics

# Acknowledgments

I would like to thank my current advisors Wolfgang Ketterle and David Pritchard. I enjoyed our conversations about physics, and I am ceaselessly amazed at both of your abilities to come up with ways any physical quantity should scale with other physical quantities (all prefactors are unity!). I will miss being on what I think is the cusp of an important experimental direction for atomic physics to take. I would also like to thank my former advisor Chris Monroe for providing one of the primary sparks for my initial interest in physics. I look forward to joining your lab, this time at a new venue. The halls of Maryland's atomic physics department will soon echo with the glorious sounds of NFL films music.

David Weld is a fantastic post doc. He has done an amazing job with the steep learning curve of BECIV, and I know he will get some nice results out of the experiment. Whenever I had a physics question, Dave immediately saw the answer and could explain it in a way that makes the result intuitively obvious. He is also the biggest Red Sox fan I have ever seen; Dave named his first child Theodore William to pay tribute to both Ted Williams and Theo Epstein (he will deny this was his intention in person). Patrick Medley is one of the only people I have met that can convince me something and its opposite are true. I have really enjoyed working with him because he is really able to step back from daily lab optical alignment activities and come up with creative solutions to everyday technical problems and to think up schemes for new physics experiments. I hope one day to find a flaw in his libertarian principles. I have also enjoyed my time talking to Hiro Miyake while the two of us tried to figure out how to make spin dependent lattices and how magnetic exchange works. I'd also like to thank him for acting as a sounding board for ideas and for me to vent some of my frustrations. Thanks again and I look forward to seeing all of the BEC4 members at conferences and hearing about how antiferromagnetic ordering was achieved.

My life at MIT would certainly been a lot more dull without my friends and roommates Parthiban Santhanam and Shawn Henderson. I'll never cease to be amazed by

Parthi's ability to rope anyone into conversations about philosophy and economics that last until 5 am. Shawn is the only person I know who would buy a cowboy hat for wearing around Boston, buy Jesus candles for impressing a date, and learn to speak "fluent" Russian for various unnamed purposes. I hope I taught both of you that hyperbole is the single greatest invention in the history of the universe. Thanks to Nabil Iqbal for correcting my pronunciation of the name "Bose." I have been correcting other people (including Wolfgang) for you, and now I will write it down. The name is pronounced like "Bo" (long o sound) "sh." Since I fulfilled my end of the bargain, you have to come up with some a new and important Hamiltonian that can be simulated with ultra cold atoms in lattices. A weekly event turned tradition that I was a part of at MIT, Cookie Monday, served as a kind of social glue that held everyone together. I got to meet lots of great people and share in the weekly tradition of eating cookies every monday night. I hope all of you enjoyed some of the "inspirational" emails I sent out.

Of course I also have to thank my two best friends Mike Reim and Dan "A10! A10! A10!" Levy. I know I'll get to see Mike more often in DC, and Dan, if you ever need to go AWOL, you can hide out in my apartment. I'd also like to thank my girl friend, Tracy Wharton, for everything. I'm not sure what awaits me in Maryland, but I'm glad you're riding shotgun.

Lastly, I'd like to thank my parents Dennis and Margo Hucul and my brother Matthew for reasons too numerous to cover in this little space.

# Contents

# List of Figures

# List of Tables

# Chapter 1

# Introduction: Magnetic Ordering and Spin Exchange

The purpose of this thesis is to explore the possibility of investigating magnetic super exchange with ultra cold atoms confined in an optical lattice. Ultra cold atoms confined in optical lattices are very much an analog of condensed matter systems. Although these systems are typically larger than lattices in solid state systems, ultra cold atoms in lattices behave in much the same way traditional condensed matter systems displaying such phenomenon as BCS superfluidity [1–5] and Mott insulation [6–9]. Many of the traditional tools of atomic physics such as state preparation and high precision spectroscopy can be combined with precise control of atomic interactions via the application of external fields. These tools offer an attractive opportunity to engineer many body Hamiltonians that are of interest in condensed matter physics for investigating strongly correlated physics and to compare experimental results of "pristine" atomic systems with first principle calculations.

Using cold atoms in optical lattices, it may be possible to simulate condensed matter systems along the lines of Feynman's original idea for analog quantum simulation: build one quantum system (cold atoms in lattices that behave according to the Bose-Hubbard model) to simulate another (solid state systems that interact via an effective Heisenberg model) [10]. Building these kinds of quantum simulators may be an important avenue for understanding strongly correlated physics and develop-

ing materials that are not well described by current mean field approaches to states of broken symmetry or Landau Fermi liquid theory of weakly interacting electron systems. Calculating the properties of even the simplest strongly correlated system models, such as magnetic properties in the Heisenberg model, is challenging. Experimentally confirming the results of some of these models is one of the major challenges of modern experimental condensed matter physics.

Currently, there are two main avenues of research that are predicated on being able to realize the Bose-Hubbard Hamiltonian: high temperature superfluidity and quantum magnetism. This thesis will deal primarily with the latter in the context of being able to observe magnetic ordering as the result of magnetic super exchange with bosons in a three-dimensional cubic lattice. A natural extension of studying magnetic super exchange with ultra cold bosons in optical lattices presented here is to use a frustrated lattice in two dimensions with antiferromagnetic interactions. These systems offer the opportunity of observing novel states of matter such as resonating valence bond states and spin liquid states, as well as possible application in fault-tolerant quantum computation [11]. Investigating these exotic spin systems may shed light on the mechanism of high temperature superconductivity.

## 1.1 Magnetic Ordering with Classical Dipolar Interactions

The semiclassical picture of magnetic ordering is one based on dipole-dipole coupling of atomic magnetic moments. What sorts of magnetic ordering are expected from such an interaction? Consider Fig. 1.1 where dipole moments are arranged in a three dimensional cubic lattice. The Hamiltonian for such as system is $H = -\mu \cdot B$, where $\mu$ is the magnetic dipole moment of the atoms and B is the local magnetic field from the surrounding magnetic dipoles. Consider populating the lattice with atoms one at a time and consider only nearest neighbor interactions.

If one atom's dipole moment points along a lattice axis, the nearest neighboring

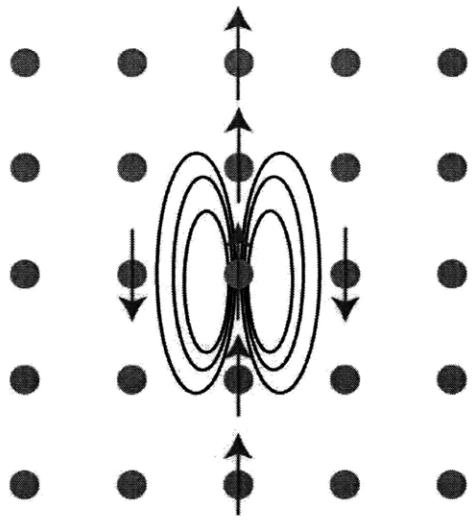

Figure 1-1: Semi classical dipole coupling between the magnetic moments of atoms to their local field. The figure depicts the predicted magnetic ordering in a cubic lattice. If the magnetic moment of the atom in the center of the array points along a lattice axis, it generates a dipole magnetic field as shown by the lines in the figure. The neighboring magnetic moments of atoms on the left and right of this central atom point in the opposite direction to minimize their interaction energy. A classical dipole coupling scheme then leads to striped antiferromagnetic ordering and excludes the ferromagnetic state as the ground state at zero temperature.

atoms align their magnetic dipole moments with the magnetic field from the first atom to minimize the energy of the configuration. Continuing to fill the lattice produces a stripped pattern of dipole moments shown in Fig. 1.1. This system is distinctly odd and does not display ferromagnetic ordering as one might naively expect. In fact, changing the above system to a ferromagnetic state costs an energy of order twice the dipole energy times half the number of atoms in the system to flip the spin of roughly half of the atoms in the system in the thermodynamic limit. Clearly, this model of magnetic ordering fails spectacularly: it expressly excludes the phenomenon of a ferromagnetic ordered ground state in the low temperature limit.

## 1.2 Curie Temperature with Classical Dipolar Interactions

Even though classical dipolar interactions forbid a ferromagnetic ground state, suppose one existed. It is possible to estimate the Curie temperature using a semiclassical model of magnetic interactions in matter [12].

$$T_c = \frac{\lambda N \mu^2}{k \epsilon_0 c^2} \tag{1.1}$$

where $\mu = e\hbar/2m$ is the magnetic moment of an electron, and $\lambda$ is an adjustable parameter that depends on geometry and is of order unity. For ferromagnetic substances like nickel, the density $N \approx 10^{30}$ m$^{-3}$, so the Cure temperature is of order 100 mK and is approximately three orders of magnitudes below observed Curie temperature. If the ordering was classical, the Curie temperature is of order the nearest neighbor dipole interaction energy, well below the observed Curie temperatures of most ferromagnets (100 - 1000 K).

A semi-classical model of magnetic ordering based on classical dipole coupling not only predicts ferromagnetic ground states do not exist, but that if one did exist, the spin ordering would melt at very low temperatures. Magnetic ordering is not a classical or semi-classical phenomenon; magnetic ordering is explained by quantum mechanics. The model typically invoked to explain magnetic ordering is the so called Heisenberg model

$$H = -J \sum_{i=x,y,z;j} \sigma_j^i \sigma_{j+1}^i - h\sigma_j^z \tag{1.2}$$

with the magnetic exchange constant J that is purely quantum mechanical in nature.

## 1.3 Quantum Magnetism and Magnetic Super Exchange

The quantum mechanical explanation for magnetic ordering generally involves two types of exchange mechanisms: direct exchange and super exchange [13]. In the direct ferromagnetic exchange case, electrons form spin symmetric states. This forces the two-electron spatial wavefunction to be antisymmetric and reduces the coulombic repulsion between the electrons, thus lowering the interaction energy. This result is derivable from first order perturbation theory and is analogous to Hund's rules for electrons in atoms. In the antiferromagnetic direct exchange case, an electron can hop to a site with anti-parallel spin, thus lowering the kinetic energy of the electron. This result is also derived from first order perturbation theory.

Magnetic super exchange is a virtual double occupation that is derivable from second order (or higher order) perturbation theory. The physical interpretation is that an electron hops to a neighboring site with anti-parallel spin, and owing to a large on site repulsion energy, hops back to its original location. This virtual double occupation process can reduce the kinetic energy of the electron system. Super exchange process will be described more fully later in this thesis (see section 2.3). This process is responsible for long range antiferromagnetic ordering in cuprate materials, which turn superconducting when doped.

## 1.4 Quantum Magnetism and High Temperature Superconductivity

The mechanism for high temperature superconductivity has been a major puzzle for several decades [14–16]. The parent compounds of the high $T_c$ cuprates are antiferromagnetic Mott insulators and in general, high $T_c$ superconducting materials are generally found close to Mott insulators with magnetic ordering. These superconducting materials have anisotropic pairing of electrons (d-wave pairing), and there

are some indications that d-wave pairing can be seen in the Hubbard model [17], a model that is connected to the Heisenberg model.

Experiments have established the proximity of the undoped Mott insulator to the doped superconductor, but there is still debate about the connection between the undoped Mott insulator and the doped superconductor [18, 19]. The Mott insulating state develops long ranged antiferromagnetic Neel ordering, but doping this insulator extinguishes the magnetic ordering and the system becomes superconducting. Current understanding suggests that doping the antiferromagnetic Mott insulator effectively frustrates the Neel order and pushes the system into a superconducting regime. Some have suggested that an understanding of the cuprate materials may come from understanding Mott insulating states with no long range magnetic order, such as spin liquids. Upon doping such nonmagnetic states, the system may become a d-wave superconductor [18, 20–24].

If this is the origin of high temperature superconductivity, realizing and studying spin liquids with cold atoms in optical lattices may prove a very fruitful avenue to understanding high temperature superconductivity. It may be possible to achieve a spin liquid with cold atoms in optical lattices by engineering antiferromagnetic interactions between atoms on a frustrated lattice such as a triangular or Kagome lattice [25].

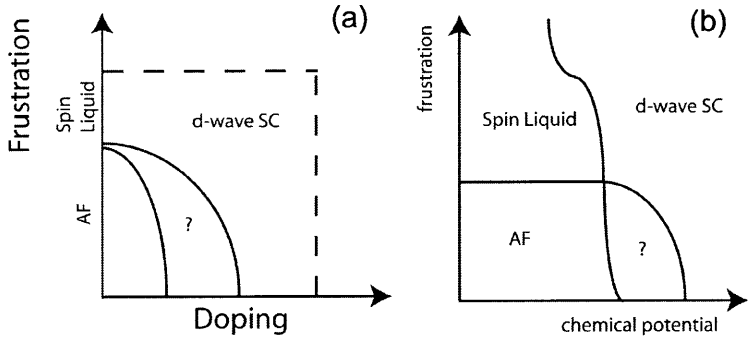


Figure 1-2: Illustration of a high $T_c$ superconductor phase diagram as a function of frustration and doping at zero temperature as suggested by [18]. The y-axis is designated by the amount of frustration in the system, while the x-axis is doping. At zero doping and finite frustration, there are at least two Mott insulating states: an antiferromagnetic state (AF) with long range Neel order, and a spin liquid state. The spin liquid state has no long range spin order but has well localized atoms at lattice sites. Doping either of these states may lead to high temperature, d-wave superconductivity (SC). Realizing antiferromagnets and spin liquids with cold atoms in lattices may lead to new discoveries about the nature of high temperature super conductivity.

# Chapter 2

# The Bose-Hubbard Hamiltonian

The Hubbard Hamiltonian is an important model used to explain a wide variety of phenomena in condensed matter physics, and its transformation to the Heisenberg Hamiltonian forms the basis of understanding magnetic super exchange ordering and predicts several exotic phases of matter such as spin liquids and valence bond states. Another main area of research is the applicability of the Hubbard model to explain high temperature superconducting materials. The Hubbard model may capture the features of d-wave pairing by considering repulsive fermions on a lattice [17].

After the realization of Bose-Einstein condensation with ultra cold alkali gases in the mid 1990s, Jaksch et al. suggested the possibility of studying the Hubbard model using cold bosons in an optical lattice to observe the superfluid to Mott insulator transition [26]. This transition was experimentally observed first by Greiner et al in 2002 [6]. The Bose-Hubbard model describes interacting bosons on a periodic lattice. The general idea is that if the lattice potential is weak enough, the bosons can tunnel from lattice site to lattice site to lower the kinetic energy of the system. However, there is a potential energy cost from particles interacting with the light field and scattering off of each other. The relative sizes of these energy terms determines the phase of the system. The Bose-Hubbard model makes a few assumptions about the energy scales involved in the system. The first is that the band gap is much larger than both the thermal and interaction energies of the particles. The second is that the Wannier functions decay rapidly compared to the lattice spacing. The Bose-Hubbard

model is

$$H = -t\sum_{ij}(a_i^\dagger a_j + a_j^\dagger a_i) + \frac{U}{2}\sum_i n_i(n_i - 1) + \sum_i \epsilon_i n_i \tag{2.1}$$

where $t$ represents the hopping matrix element and $U$ is the potential enegy. The $\epsilon_i$ term is included because focusing light on atoms produces a slowly varying trapping potential as a function of space. This term acts like a spatially dependent chemical potential. In the $\epsilon_i = 0$ limit, the Bose-Hubbard model has two terms that compete to determine the state of the system: the kinetic energy term $t$ favors particle delocalization while the potential energy $U$ term that favors one particle per site. By adjusting the laser intensity of an optical lattice confining the bosons, it is possible to tune the ratio $U/t$ and thus go from a localized, Mott insulating state with an integer number of particles per site, to a delocalized superfluid state. This is the superfluid to Mott insulator quantum phase transition within the context of the Bose-Hubbard model as worked out by Fisher et al [27].

## 2.1 From a weakly interacting quantum gas to the single component Bose-Hubbard model

Now we want to derive the Bose-Hubbard model starting from the Hamiltonian describing a weakly interacting quantum gas of bosons. The Hamiltonian for a weakly interacting quantum gas of bosons is [28]

$$H = \int d^3x \Psi^\dagger(x)\Big(\frac{p^2}{2m} + V(x) + U_T(x)\Big)\Psi(x) + \frac{4\pi a_s}{2m}\int d^3x \Psi^\dagger(x)\Psi^\dagger(x)\Psi(x)\Psi(x) \tag{2.2}$$

In the above equation, $\Psi$ ($\Psi^\dagger$) is the bosonic field destruction (creation) operator for a single boson in state $|a\rangle$ at the position x. For multicomponent system, the field operators can be summed over the various states $|\phi_i\rangle$. A slowly varying external trapping potential $U_T(x)$ compared to the period of the lattice is included and can be the result of an external applied magnetic field or from the envelope of focused laser beams that define an optical lattice. The s-wave scattering length is given by

$a_s$. In the ultra cold regime, the bosonic system is well approximated by a single band model, so the bosonic field operators can be expanded in terms of creation and destruction operators at individual lattice sites multiplied by the appropriate Wannier functions centered at each lattice site $x_i$.

$$\Psi(x) = \sum_i a_i w(x - x_i) \tag{2.3}$$

The Hamiltonian now reads:

$$H = -\sum_{ij} t_{ij}(a_i^\dagger a_j + a_j^\dagger a_i) + \frac{1}{2}\sum_{ij,\sigma} U_{ijkl} a_i^\dagger a_j^\dagger a_j a_i \tag{2.4}$$

where the coefficients $t_{ij}$ and $U_{ij}$ are given by:

$$t_{ij} = -\int d^3x w(x - x_i)\Big(\frac{p^2}{2m} + V(x) + U_T(x)\Big)w(x - x_j) \tag{2.5}$$

$$U_{ij} = \frac{4\pi a_s}{m}\int w^2(x - x_i)w^2(x - x_j) \tag{2.6}$$

Since the Wannier functions are orthogonal, and assuming an isotropic, deep lattice and neglecting next nearest neighbor interactions, then the $U_{ij}$ can be replaced by $U_\sigma$ and can be interpreted as an onsite interaction while $t_{ij} = t$, the tunneling matrix element. Adding the trapping potential back in yields the Bose-Hubbard Hamiltonian for a single component bosonic system in a lattice

$$H = -t\sum_{\langle ij\rangle} a_i^\dagger a_j + a_j^\dagger a_i + \frac{U}{2}\sum_i n_i(n_i - 1) + \sum_i \epsilon_i n_i \tag{2.7}$$

## 2.2 Phases of the single component Bose Hubbard Hamiltonian

It is difficult to solve Eq. 2.7 exactly for all ratios $t/U$, although the features of this model and the properties of the quantum phase transition have been worked out as a function of $t/U$ [27]. In the limit $U/t = 0$, the many particle wave function is

delocalized to lower the kinetic energy of the system. The system is an ideal BEC, and in the limit $U/t \rightarrow 0$, the ground state of the Bose Hubbard Hamiltonian is a Gross-Pitaevskii state with a condensate fraction that approaches unity ($U/t = 0$ is an ideal BEC). In the thermodynamic limit, the state of the system can be thought of as a collection of local coherent states at each lattice site with average occupancy $\langle n \rangle = N/N_L$ where N is the number of atoms and $N_L$ is the number of lattice sites [29]. In the opposite limit, $t/U = 0$, the atoms minimize their energy by fixing the number of particles per lattice site to an integer value; the system is a Mott insulator. Including the effect of the effective chemical potential from an overall (approximately) harmonic external confinement, the insulator develops a "wedding cake" structure with an integer number of particles per lattice site that decreases in a stepwise fashion as one moves toward the edge of the cloud. This transition, including the wedding cake structure, has been observed experimentally [6, 8, 9]. More detailed information about this phase diagram can be found in [29] and the references therein.

## 2.3 Two component Bose Hubbard model

If there is one type of boson in an optical lattice in two different hyperfine levels, Eq. 2.7 should be modified to include the tunneling of both species individually, as well as both inter- and intra- component interactions $U_a$, $U_b$, and $U_{ab}$. The two component Bose-Hubbard model is [25, 30]

$$H = -\sum_{\langle ij \rangle} t_a(a_i^\dagger a_j + a_j^\dagger a_i) + t_b(b_i^\dagger b_j + b_j^\dagger b_i) + U_{ab}\sum_i n_{ai}n_{bi} + \frac{1}{2}\sum_{i,\sigma=a,b} U_\sigma n_{i\sigma}(n_{i\sigma}-1) - \sum_{i\sigma}\epsilon_{i\sigma}n_{i\sigma} \tag{2.8}$$

The last term $\epsilon_{i\sigma}$ arises from an additional trapping potential and $\sigma = a, b$ refers to the two atomic hyperfine levels. If there is no transfer between the two different hyperfine levels, the magnetization $(n_a - n_b)$ is conserved. The magnetization of the sample can be used to set the effective chemical potentials for the two component bosonic system.

As pointed out by Duan et. al [25] and E. Altmann et. al [30], it is possible

in principle to control the tunneling rates and interaction energies of cold atoms in an optical lattice by making a state dependent optical lattice. The state dependent optical lattice can be used to control spin dependent tunneling and interaction energies of a two species ultra cold atomic system. This magnetic super exchange energy allows one to control the exchange energy of the Heisenberg Hamiltonian which opens up the possibility of studying magnetic ordering at the quantum level. This Hamiltonian (Eq. 2.8) has a number of interesting insulating phases when $U \gg t$. The tunneling term $t$ is a small perturbation in this regime, and perturbation theory illuminates the effective Hamiltonian of this system. Using the Schrieffer-Wolf transformation or other methods [25, 30, 31], the two bosonic species Hamiltonian is equivalent to the following Heisenberg Hamiltonian to leading order in $t^2/U$

$$H = \sum_{\langle ij \rangle} \lambda_z \sigma_i^z \sigma_j^z - \lambda_\perp (\sigma_i^x \sigma_x^z + \sigma_i^y \sigma_j^y) \tag{2.9}$$

neglecting a term proportional to $t^2/U \cdot \sigma^z$ that can be canceled with an applied magnetic field. The effective z-spin operator is related to the operators in the two species Bose Hubbard model by $\sigma_i^z = a_{ia}^\dagger a_{ia} - a_{ib}^\dagger a_{ib} = n_{ia} - n_{ib}$, the difference between the number of atoms in state "a" and the number of atoms in state "b." The x and y spin operators are given by $\sigma_i^x = a_{ia}^\dagger a_{ib} + a_{ib}^\dagger a_{ia}$ and $\sigma_i^y = -i(a_{ia}^\dagger a_{ib} - a_{ib}^\dagger a_{ia})$. Since the commutator $[a_i^\dagger, a_j] = \delta_{ij}$, it is easy to show that the effective spin operators obey the commutation relation $[\sigma^i, \sigma^j] = i\epsilon_{ijk}\sigma^k$ The coefficients $\lambda_z$ and $\lambda_\perp$ are given by [25]:

$$\lambda_z = \frac{t_a^2 + t_b^2}{2U_{ab}} - \frac{t_a^2}{U_a} - \frac{t_b^2}{U_b} \tag{2.10}$$

$$\lambda_\perp = \frac{t_a t_b}{U_{ab}} \tag{2.11}$$

Although a more complicated process is necessary to calculate the coefficients $\lambda_\perp$ and $\lambda_z$, it is possible to understand the magnitude and sign of these coefficients using second order degenerate perturbation theory. In the insulating limit, take the zeroth order Hamiltonian to have only the interaction terms proportional to $U_\sigma$ and $U_{ab}$.

The state of the system is an insulator with either a single single atom in hyperfine state $|a\rangle$ or in state $|b\rangle$ at every lattice site. The energy of this system is zero and has high degeneracy. For simplicity, consider a two site, two atom, single band model. The matrix elements of the degenerate Hamiltonian are

$$\langle\alpha|H^{(2)}|\beta\rangle = -\sum_n \frac{\langle\alpha|H^{(hop)}|n\rangle\langle n|H^{(hop)}|\beta\rangle}{\langle n|H^{(0)}|n\rangle} \tag{2.12}$$

where $|\alpha\rangle$ and $|\beta\rangle$ are the possible insulating states in the Hilbert space of the system and $H^{hop}$ is the perturbing Hamiltonian: the hopping terms in Eq. 2.8 . In this case, there are four possible states because there are two sites with two internal states. The hopping matrix can tunnel a boson of either hyperfine state from lattice site to another, but upon doing so, the other hopping matrix element should make a boson hop back to the empty lattice site to ensure there is only one boson per lattice site. The order of the degenerate Hamiltonian's matrix elements is therefore $-t^2/U$. Since bosons can be in the same quantum state, a boson can hop from one lattice site to a neighboring site with a boson in the same hyperfine state. The boson can then hop back to its original site, resulting in a reduction of the kinetic energy by an amount $t_\sigma^2/U_\sigma$. Since there are two hyperfine species, either one can undergo this process. This stimulative term (reduction of the energy of the system from having alike hyperfine species neighbors) drives z-ferromagnetic ordering of bosons in three dimensional, cubic optical lattices. Neighboring bosonic atoms with opposite spins can also tunnel to adjacent lattice sites and tunnel back, resulting in a kinetic energy decrease of order $t_\sigma^2/U_{ab}$ (the negative sign is picked up by the spin operators $\sigma_z$). This antiferromagnetic term drives the bosons confined in a cubic, three dimensional lattice to adopt classical Neel antiferromagnetic ordering. Finally, a boson in a particular hyperfine state can hop to its neighboring site and the opposite hyperfine state neighbor can hop to fill the newly created hole. This reduces the kinetic energy by an amount of order $t_a t_b/U_{ab}$ and drives bosonic atoms to adopt XY ferromagnetic order.

In the case of fermions, there is no stimulative term because a fermion hopping to an adjacent site in the same hyperfine state would violate the Pauli exclusion principle.

Fermionic atoms can hop to an adjacent site with opposite spin and hop back, lowering the kinetic energy and driving the system to adopt classical Neel antiferromagnetic ordering in the three dimensional cubic lattice. Like bosons, fermions in a particular hyperfine state can also hop to a neighboring site in the opposite hyperfine state, and the neighbor can hop back to fill the newly created hole. However, there is a minus sign in front of $\lambda_\perp$ in the case of fermions because of the antisymmetry requirements. This drives the fermionic atoms to adopt XY Neel order instead of XY ferromagnetic order as in the case of bosonic atoms.

Without the second order process of virtual occupation of lattice sites, called magnetic super exchange, a disordered system (random distribution of hyperfine states amongst the singly occupied sites) would not order. The competition between $-(t_a^2 + t_b^2)/U_{ab}$ and $-t_\sigma^2/U_\sigma$, and $t_a t_b/U_{ab}$ allows for different possible orderings of the atoms in the lattice. The atoms can adopt z Neel order and XY ferromagnetic ordering in addition to z ferromagnetic order [25, 30]. Note that it is possible to observe magnetic super exchange without making spin dependent lattices. The magnetic super exchange mechanism will cause a two component bosonic system to adopt ferromagnetic ordering.

## 2.4 Phases of the the two component Bose Hubbard model

The phase diagram of a two component, Bose Hubbard Hamiltonian displays a lot of rich physics, the first of which is magnetic super exchange. This virtual double occupation process is responsible for determining various magnetic phases that are possible in the Heisenberg model. The phases are essentially controlled by the relative sizes of the first term in the expression for $\lambda_z$ (the antiferromagnetic term), the second two terms (the stimulative terms) of $\lambda_z$ and finally $\lambda_\perp$ (the XY term). It is possible to get a qualitative sense for which magnetic phase appears within the parameter space of $t$, $U_\sigma$, and $U_{ab}$ by simply comparing the antiferromagnetic term, the bosonic

stimulation term, and the XY term. In the limit the antiferromagnetic term is much larger than the bosonic term, the inter species interaction energy must be much smaller than the intra-species interaction energy: $U_{ab} \ll U_\sigma$. If the antiferromagnetic term is much larger than the XY term, there must be a tunneling asymmetry between the two hyperfine species: $t_a \neq t_b$. If these conditions hold, the system is a z-ordered Neel antiferromagnet. In order for the system to display ferromagnetic behavior along the z-axis, the bosonic stimulation term should be larger than the antiferromagnetic term and the XY term. This occurs when the inter and intra species interaction energies are approximately equal ($U_{ab} \approx U_\sigma$) and there is some tunneling asymmetry. When the XY term dominates, the system is an XY ferromagnet. As pointed out by Duan et al [25], a useful way to parameterize these ideas is to define a tunneling asymmetry

$$\beta = \frac{t_a}{t_b} + \frac{t_b}{t_a} \tag{2.13}$$

for the two component system. Note the minimum value this can take is 2. The relative sizes of $\lambda_z$ and $\lambda_\perp$ change when $\beta = \pm(1/2 - U_{ab}/U_\sigma)^{-1}$ [25], so it is possible to use this requirement as an approximation for the phase boundaries as is shown in Fig. 2.4.

There are other magnetic phases possible as well. For example, in the limit of zero tunneling of one species, $\lambda_\perp = 0$ and the Hubbard Hamiltonian becomes an Ising Hamiltonian. The application of an external magnetic field can cause first order spin-flop transitions between the antiferromagnetic phase and a canted phase (a phase with finite polarization in the z-direction and ferromagnetic order in the xy plane) [32] at a critic field $h_z = Z(\lambda_z^2 - \lambda_\perp^2)^{1/2}$ (Z is the number of nearest neighbors at each lattice site). There is also a second order transition from the XY ferromagnetic phase to a z-polarized phase at $h_z = Z(\lambda_z + \lambda_\perp)$.

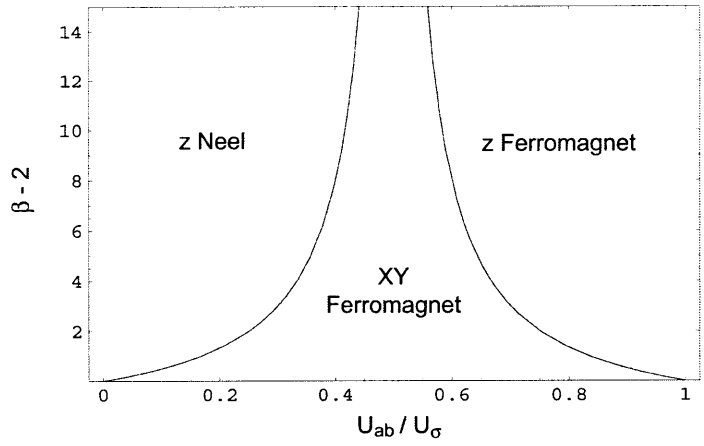


Figure 2-1: Bose Hubbard phase diagram of a two component bosonic system. The vertical axis measures the tunneling asymmetry between the two component bosonic species and is defined as $\beta = t_a/t_b + t_b/t_a$. The horizontal axis measures the ratio of the interspecies interaction energy to the intra-species interaction energy. If the inter and and intra species interaction energies are equal, the system is a z-ordered ferromagnet as a result of bosonic stimulation. If the inter species interaction energy is much higher than the intra species interaction energy, the magnetic super exchange mechanism will force the bosons to form a z-Neel antiferromagnet for adequate tunneling asymmetry. If the inter and intra species interaction energies are equal, the system will form an XY ferromagnet as a result of magnetic super exchange.

## 2.5 General interactions of cold bosons in optical lattices

There are other types of interactions that are realizable with ultra cold atoms in optical lattices by applying magnetic fields, electric fields, and radiation fields [11]. The application of these additional fields modifies the Bose-Hubbard Hamiltonian above.

$$H = H_{hop} + H_{int} + H_{mag} + H_{elec} + H_{rad} \tag{2.14}$$

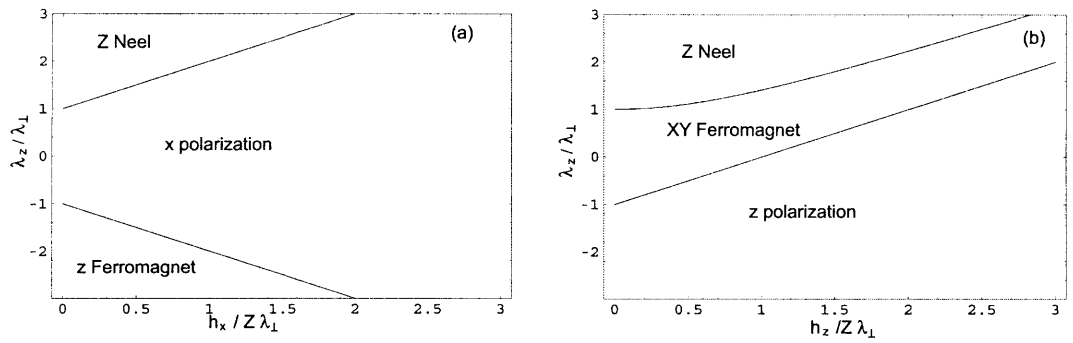


Figure 2-2: Bose Hubbard phase diagram of a two component bosonic system with applied external magnetic fields in the x (Fig. 2.2a) and z (Fig. 2.2b) directions. The vertical axis measures the ratio of the Heisenberg spin spin coupling in the z direction to the coupling in the XY plane in both plots. The horizontal axis measures the ratio of the field coupling in either the x or y direction to the XY ordering term. The phases are as marked in each diagram.

If an optical lattice confines two hyperfine levels of a single atomic species, the hopping and interaction parts of the Hamiltonian are

$$H_{hop} = \sum_{\langle ij \rangle} t_a(a_i^\dagger a_j + a_j^\dagger a_i) + t_b(b_i^\dagger b_j + b_j^\dagger b_i) \tag{2.15}$$

$$H_{int} = \sum_i \frac{1}{2}U_{aa}a_i^\dagger a_i^\dagger a_i a_i + \frac{1}{2}U_{bb}b_i^\dagger b_i^\dagger b_i b_i + U_{ab}a_i^\dagger b_i^\dagger b_i a_i \tag{2.16}$$

$$H_{hop} + H_{int} = \sum_{\langle ij \rangle} \Big( - \lambda^\perp(\sigma_i^x\sigma_j^x + \sigma_i^y\sigma_j^y) + \lambda^z\sigma_i^z\sigma_j^z \Big) + \sum_i h_z\sigma_i^z$$

where the sum runs over the lattice sites $i$ and $j$ and assumes nearest neighbor interactions after transforming to the Heisenberg model. The effective magnetic field $h_z$ is equal to $t_b^2/U_b - t_b^2/U_b$ and vanishes for maximally stretched hyperfine states. The other terms in the Hamiltonian can be expressed as

$$H_{mag} = \sum_i \epsilon(a_i^\dagger a_i - b_i^\dagger b_i) \tag{2.17}$$

$$H_{elec} = \sum_i \gamma(a_i^\dagger a_i + b_i^\dagger b_i) \tag{2.18}$$

$$H_{laser} = \sum_i \frac{\Omega}{2}(a_i^\dagger b_i e^{i\phi} + b_i^\dagger a_i e^{-i\phi}) \tag{2.19}$$

where the coefficients $\epsilon$ and $\gamma$ parameterize the Zeeman and Stark shifts from the application of magnetic and electric fields respectively to atoms in hyperfine levels $|a\rangle$ and $|b\rangle$. The term $H_{rad}$ represents the interaction of the two hyperfine levels with a plane wave that connects the two hyperfine levels. In principle one could consider the coupling of each hyperfine level to all other levels, modifying the Rabi frequency $\Omega$. The introduction of a radiation field is important because all other terms conserve the magnetization $(n_a - n_b)$ of the system while the radiation field does not. It is possible to re-write the radiation field as proportional to an effective magnetic field in the x and y directions.

$$H_{rad} = \frac{\Omega}{2} \sum_i \cos(\phi)\sigma_i^x + \sin(\phi)\sigma_i^y \tag{2.20}$$

Adding an electric field gradient to the system effectively changes the pseudo spin interaction energies [11]. For example, if an electric field gradient is added, the Stark shift term $\gamma = \gamma_0 + \eta \times k$, then the pseudo spin interactions energies are modified as follows:

$$U_{\alpha\beta} \rightarrow \frac{U_{\alpha\beta}^2 - \eta^2}{U_{\alpha\beta}} \tag{2.21}$$

For small magnetic field gradients compared to the pseudo spin interaction energies, the Zeeman term in the Hamiltonian is $\epsilon = \epsilon_0 + \nu \times k$, and the resulting effective magnetic field in the z direction becomes

$$h_z = \epsilon_0 + \frac{t_b^2 U_{bb}}{U_{bb}^2 - \nu^2} - \frac{t_a^2 U_{aa}}{U_{aa}^2 - \nu^2} \tag{2.22}$$

Using these tools, it is possible to engineer a wide variety of bosonic Heisenberg Hamiltonians because the constants in front of the spin operators are all experimental control parameters. Furthermore, it is possible to apply effective vector fields along the x, y, and z directions using electric, magnetic, and radiation fields. The full Hamiltonian that can be simulated with two component cold bosons in an optical

lattice is then:

$$H = \sum_{\langle i,j \rangle} \lambda^z \sigma_i^z \sigma_j^z - \lambda^\perp (\sigma_i^x \sigma_j^x + \sigma_i^y \sigma_j^y) + \sum_i \overrightarrow{h}_i \cdot \overrightarrow{\sigma}_i \tag{2.23}$$

with the parameters $\lambda_\perp$, $\lambda_z$ and the three components of the effective magnetic field $\overrightarrow{h}$ all adjustable by the experimenter. Exploring the phase diagram of this Hamiltonian may offer key insights in condensed matter physics and may serve as a useful tool for making controlled-phase gates: a universal gate that may prove useful for quantum computation [11, 33].

# Chapter 3

# Realizing Magnetic Super Exchange with Ultra Cold Atoms

The purpose of this section is to illuminate the construction of a spin dependent optical lattice for bosons (and especially Rb) as a means to engineer the tunneling and interaction energies associated with the effective Heisenberg model. Rb atoms have Feshbach resonances, so in principle their scattering lengths are tunable with externally applied fields, but the applied fields necessary to tune the scattering length are large. Another way to change the interaction energies is to engineer a spin dependent lattice where the atoms are slightly displaced from the electric field maxima or minima in a direction that depends on their hyperfine states.

Consider a standing light wave with linear polarization. This light wave may be decomposed in to an equal superposition of a lattice with $\sigma^+$ polarization and a lattice with $\sigma^-$ polarization. These lattices form periodic potentials for atoms, and the potential minima can be shifted with respect to each other as will be described in section 3.2. Consider what this does to the atomic interaction energies. In Fig. 3, an atom in a particular hyperfine state (depicted in blue as spin up in the center of the lattice) virtually tunnels to the right and interacts with another "spin up" atom. These atoms are virtually located at the same point in space, so they interact with an energy $U_a$. Now consider a virtual tunneling event from the center atom to the left, "spin down" atom. Upon virtual occupation of the site to the left, the spin up

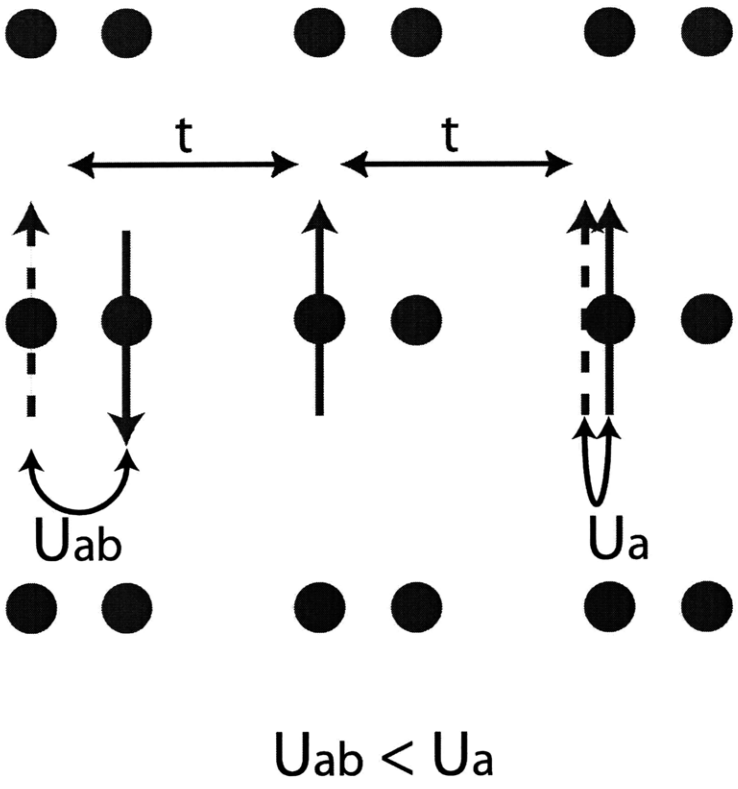


Figure 3-1: A spin dependent lattice based on moving lattice minima for different hyperfine species apart. An atom in a particular hyperfine state (depicted in blue as spin up in the center of the lattice) virtually tunnels to the right and interacts with another "spin up" atom (depicted in red). These atoms are virtually located at the same point in space, so they interact with an energy $U_a$. Now consider a virtual tunneling event from the center atom to the left, "spin down" atom. Upon virtual occupation of the site to the left, the spin up atom is slightly displaced in space from the spin down atom. These atoms interact with energy $U_{ab}$, but since their wavefunctions overlap less, this interaction energy is less than $U_a$.

atom is slightly displaced in space from the spin down atom. These atoms interact with energy $U_{ab}$, but since their wavefunctions overlap less, this interaction energy is less than $U_a$. Displacing the lattice minima of the two hyperfine species thus lowers the ratio $U_{ab}/U_\sigma$ and drives the system to adopt antiferromagnetic ordering in the limit $U_{ab}/U_\sigma \rightarrow 0$ if there is spin dependent tunneling.

## 3.1 Magnetic Super Exchange in non-Spin Dependent Lattices

First, consider the possibility of seeing super exchange in a lattice with no spin dependence. The two component Bose Hubbard Hamiltonian is equivalent to an effective Heisenberg Hamiltonian for bosons confined to an optical lattice in the Mott insulating regime. The Heisenberg Hamiltonian is

$$H = \sum_{\langle ij \rangle} \lambda_z \sigma_i^z \sigma_j^z - \lambda_\perp (\sigma_i^x \sigma_x^z + \sigma_i^y \sigma_j^y) \tag{3.1}$$

with coefficients

$$\lambda_z = \frac{t_a^2 + t_b^2}{2U_{ab}} - \frac{t_a^2}{U_a} - \frac{t_b^2}{U_b} \tag{3.2}$$

$$\lambda_\perp = \frac{t_a t_b}{U_{ab}} \tag{3.3}$$

where $t_{a,b}$ is the spin dependent tunneling energy of hyperfine species $|a\rangle$ and hyperfine species $|b\rangle$ and $U_{a,b}$ and $U_{ab}$ are the intra and inter species interaction energies respectively. In the absence of any difference in the tunneling or interaction energies of the hyperfine species, the resulting Hamiltonian is

$$H = -\frac{t^2}{U} \sum_{\langle ij \rangle} S_i \cdot S_j \tag{3.4}$$

This Hamiltonian displays ferromagnetic ordering with exchange constant $t^2/U$ as a result of magnetic super exchange. If cold bosons are in a random, incoherent mixture of hyperfine levels and are confined to an optical lattice that has no spin dependence, they will order ferromagnetically. Since the overall magnetization $(n_a - n_b)$ of the system is conserved, a random collection of hyperfine states will form ferromagnetic domains in the limit of a vanishing applied external magnetic field in the xy-plane.

There are inevitably uncontrolled magnetic field gradients present in labs at the $10^{-3}$ G/cm level. For alkali atoms like Rb, the Zeeman energy is of order 1 MHz/G,

so assuming a magnetic field gradient of $10^{-3}G/cm$, the energy shift across the cloud is of order 0.1 Hz /$\mu$m or about 0.05 Hz across a lattice site with a lattice constant of 500 nm. This energy scale is more than an order of magnitude below the super exchange energy ($\approx$ 1 Hz) for Rb confined in an optical lattice in a Mott insulating state. By controlling ambient magnetic field gradients, magnetic ordering should be controlled by the magnetic super exchange mechanism and not the Zeeman energy. The Zeeman energy may control the formation of ferromagnetic domain boundaries as the Zeeman energy shift from ambient magnetic field gradients becomes comparable to the super exchange energy across tens of lattice sites. The magnetic super exchange mechanism should be manifested as ferromagnetism with bosons confined in an optical lattice with no spin dependence.

## 3.2 Spin Dependent Optical Lattices

An optical lattice can be formed from two linearly polarized counterpropagating beams that constructively interfere to make a standing wave. This standing light wave can be decomposed in to an equal superposition of $\sigma^+$ and $\sigma^-$ circular polarized lattices. If the two counter propagating beams' polarization directions are at an angle $\phi$ with respect to each other, the resulting light intensity pattern is $I = I^+ \cos^2(kx + \phi/2) + I^- \cos^2(kx - \phi/2)$. These two independent, circularly polarized lattices are displaced from each other in space with the separation dictated by the angle $\phi$ by $\Delta x = \phi/k = \phi\lambda/2\pi$. If $\phi = 0$, the lattice minima of both lattices are on top of each other. As the angle $\phi$ is increased, the lattice separation increases until $\phi = \pi/2$. At this angle the lattice separation reaches a maximum value $\lambda/4$, corresponding to half of the lattice period $\lambda/2$. Atoms in two different spin states confined in such an optical standing wave experience a spin dependent lattice if the two circular polarizations couple differently to the two different states. For example, consider the following two $|F, m_F\rangle$ hyperfine states of $^{87}$Rb: $|a\rangle = |2, 2\rangle$ and $|b\rangle = |1, -1\rangle$. The dipole potential for each species with $\lambda = 785$ nm is $V_a^- \cos^2(kx - \phi/2)$ and $V_b = V_b^- \cos^2(kx - \phi/2) + 3/4V_b^+ \cos^2(kx + \phi/2)$ for states $|a\rangle$ and $|b\rangle$ respectively.

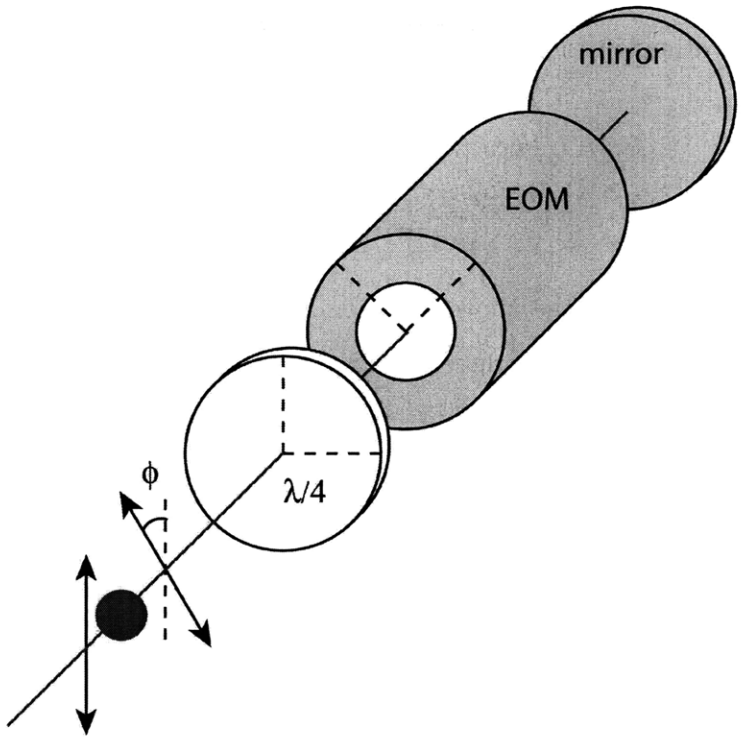


Figure 3-2: Experimental setup for tuning the angle $\phi$ in a spin dependent lattice in a one dimension. Linearly polarized light is incident on a BEC, represented by a red dot in the figure. The light continues through a quarter-wave plate and passes through an electro-optic modulator (EOM). The mirror retro-reflects the light where it passes back through the EOM and quarter-wave plate. The counter-propagating light that reaches the BEC is rotated by an angle $\phi$ which can be adjusted by use of the EOM and quarter-wave plate. The resulting standing light wave can be written as a superposition of two circularly polarized lattices with intensity extrema that are separated from each other by a distance $\Delta x = \phi\lambda/2\pi$.

Experimentally, it is possible to tune the angle $\phi$ by using one retro reflected beam that travels through a quarter wave plate and an electro-optic modulator (see Fig. 3.2.) [34] By controlling the applied voltage to the EOM, it is possible to change $\phi$.

The resulting potential for an atom in hyperfine state $|a\rangle$ confined in this optical potential is

$$U = U_a^+ \cos^2(kz + \phi/2) + U_a^- \cos^2(kz - \phi/2) \tag{3.5}$$

with the plus and minus superscripts referring to light shift from $\sigma^+$ and $\sigma^-$ polariza-

tions. If there are two different hyperfine species (hyperfine state $|a\rangle$ and hyperfine state $|b\rangle$) of atoms in the optical potential, then the potentials for each atom are

$$U_a = U_a^+ \cos^2(kx + \phi/2) + U_a^- \cos^2(kx - \phi/2) \tag{3.6}$$

$$U_b = U_b^+ \cos^2(kx + \phi/2) + U_b^- \cos^2(kx - \phi/2) \tag{3.7}$$

None of coefficients in the above equation are necessarily equal to each other. However, by choosing the appropriate hyperfine states, it is possible to make one hyperfine state interact more strongly with $\sigma^+$ polarized light and the other hyperfine state interact more strongly with $\sigma^-$ polarized light. The potential minima of these two hyperfine states are separated from each other by an amount dictated by the phase $\phi/2$ and the coefficients $U_{a,b}^{\pm}$. This separation of the hyperfine species near a lattice site allows for control of the interaction term $U_{ab}$ in the two component Heisenberg Hamiltonian. Experimentally, by adjusting $\phi$, the laser intensity, and the laser detuning, it is possible to tune the ratio of $U_{ab}/U_\sigma$ as well as the differential tunneling to explore the phase diagram of the Heisenberg Hamiltonian.

Consider the potential that confines an atom in hyperfine state $|a\rangle$ in Eq. 3.6. This potential may be re-written in the form of a DC offset plus two oscillatory functions.

$$U_a = \frac{U_a^+ + U_a^-}{2} + \frac{U_a^+ + U_a^-}{2}\cos(\phi)\cos(2kx) + \frac{U_a^- - U_a^+}{2}\sin(\phi)\sin(2kx) \tag{3.8}$$

This equation can be rewritten again as a DC offset and one oscillatory function

$$U_a = \frac{U_a^+ + U_a^-}{2} + U_d \cos(2kx - \beta) \tag{3.9}$$

$$U_d = \frac{1}{2}\sqrt{(U_a^+)^2 + (U_a^-)^2 + 2(U_a^+)(U_a^-)\cos(\phi)} \tag{3.10}$$

$$\beta_a = \tan^{-1}\Big(\frac{U_a^- - U_a^+}{U_a^- + U_a^+}\tan(\phi)\Big) \tag{3.11}$$

where $V_d$ is the lattice depth. The potential for $U_b$ is of the exact same form as $U_a$

with all subscripts replaced. The two different atoms are thus separated by a distance

$$\Delta x = \frac{|\beta_b - \beta_a|}{2k} \tag{3.12}$$

Note that since each of the coefficients $U^{\pm}_{a,b}$ should be linearly proportional to the light intensity. The separation of the hyperfine species therefore does not depend on the laser power because $\beta_{a,b}$ depends on the ratio of linear combinations of $U_{a,b}$. The angle $\phi$, the laser frequency, and dipole moments of the atoms determine the separation of the lattice minima of the hyperfine species.

The ratio of the inter species interaction energy to the intra species interaction energy $U_{ab}/U_\sigma$ can be explicitly calculated in terms of $\Delta x$. In the deep lattice limit (well defined number state), the atomic wave functions at each site can be approximated as Gaussians, so Wannier functions can be replaced with Gaussian wavefunctions

$$w(x) \approx \left(\frac{1}{2\pi\sigma^2}\right)^{1/4} e^{-\frac{(x-x_0)^2}{4\sigma^2}} \tag{3.13}$$

with $\sigma^2 = \hbar/2m\omega$ so the individual wave functions on each lattice site are normalized. The trap frequency $\omega$ is related to the trap depth $V_d$ (defined by Eq. 3.10) by $\omega^2 = 4E_R V_d/\hbar^2$ where $E_R = \hbar^2 k^2/2m$ is the recoil energy. The pseudo spin interaction energy between two unlike pseudo spins is proportional to the overlap of two Gaussian wavefunctions. If atoms in states $|a\rangle$ and $|b\rangle$ are separated by a distance $\Delta x$, then the interaction energy is

$$U_{ab} \propto \langle \psi_a^\dagger \psi_b^\dagger \psi_b \psi_a \rangle = \frac{1}{2\pi\sigma^2} \int_{-\infty}^{\infty} e^{-\frac{x^2}{2\sigma^2}} e^{-\frac{(x-\Delta x)^2}{2\sigma^2}} dx = \frac{e^{-\Delta x/4\sigma^2}}{\sqrt{4\pi\sigma^2}} \tag{3.14}$$

The pseudo spin interaction energy between $|a\rangle$ and $|a\rangle$ atoms is proportional to

$$U_{aa} \propto \langle \psi_a^\dagger \psi_a^\dagger \psi_a \psi_a \rangle = \int_{-\infty}^{\infty} |w(x)|^4 dx = \frac{1}{\sqrt{4\pi\sigma^2}} \tag{3.15}$$

The ratio of the pseudo spin interaction energies is

$$\frac{U_{ab}}{U_\sigma} = e^{-\Delta x^2/2\sigma^2} = e^{-m\Delta x^2\sqrt{V_d E_R}/\hbar^2} \tag{3.16}$$

For fixed lattice depth, the ratio of the spin interaction energies can vary wildly by increasing the separation $\Delta x$ between $|a\rangle$ and $|b\rangle$ atoms on a single lattice site.

## 3.3 Calculating the Spin Dependent Potentials

Calculating the required intensity as a function of wavelength to produce a particular ratio of inter to intra species interaction energies requires the calculation of the spin dependent potentials. In order to calculate the required intensities, we will select a desired ratio of the intra to inter species interaction energy and fix the lattice depth $V_d = N_R E_R$ so the two component system is in the Mott insulation regime (for example- Rb confined in an optical lattice of depth 15 $E_R$ is a Mott insulator). The intensity comes from Eqn. 3.10 if $\phi$ is known after fixing the lattice depth. The angle $\phi$, like Eqn. 3.10, requires calculation of the spin dependent coefficients $U^{\pm}_{a,b}$.

In atomic two-level systems, the spin dependent potential coefficients $U^{\pm}_{a,b}$ come from the appropriate atomic levels coupling to the light that forms the optical lattice. We will see that for certain states in atomic systems, the differential coupling of two atomic states to the $\sigma^{\pm}$ polarization states of light will lead to a different potential for the two atomic states as the result of differing AC Stark shifts. For an atom interacting with light, the AC stark shift is written as

$$U = -\frac{1}{4}\alpha(\omega)E_0^2 \tag{3.17}$$

where $\alpha(\omega)$ is the atomic polarizability and $E_0$ is the amplitude of the electric field. The atomic polarizability is

$$\alpha(\omega) = \frac{2e^2}{\hbar}\frac{\omega_0}{\omega_0^2 - \omega_L^2}|\langle a|z|b\rangle|^2 \tag{3.18}$$

where $\omega_0$ is the resonance frequency, $\omega_L$ is the laser frequency, and $|\langle a|z|b\rangle|^2$ is the oscillator strength. The Rabi frequency is $\omega_R = \langle a|z|b\rangle eE_0/\hbar = E \cdot D/\hbar$ with the dipole moment $D$. The laser intensity is the product of the electromagnetic energy density and the wave velocity, so $I = c\epsilon_0 E^2/2$. The spin dependent potential can then be written as

$$U_a = -\frac{ID_-^2}{2\epsilon_0\hbar c}\Big(\frac{-1}{\Delta} + \frac{1}{\Sigma}\Big)\cos^2(kz - \phi/2) + -\frac{ID_+^2}{2\epsilon_0\hbar c}\Big(\frac{-1}{\Delta} + \frac{1}{\Sigma}\Big)\cos^2(kz + \phi/2) \quad (3.19)$$

where $\Delta = \omega_L - \omega_0$ is the detuning and $\Sigma = \omega_L + \omega_0$. This equation should actually be summed over all possible transitions with the appropriate Clebsch-Gordan coefficients; the coefficient in front of $\cos^2(kz - \phi/2)$ should be summed over all possible $\sigma^-$ transitions. The coefficient in front of $\cos^2(kz + \phi/2)$ should be summed over all possible $\sigma^+$ transitions.

As a concrete example, consider the $S_{1/2}$ ground state of rubidium atoms in the $|F, m_F\rangle = |1, -1\rangle$ hyperfine state. Linearly polarized light is an equal superposition of $\sigma^+$ and $\sigma^-$ polarizations, so the light can couple to the F = 2 and F = 1 manifolds in the $P_{1/2}$ state (the D1 transition) and the F = 0, 1, and 2 manifolds of the $P_{3/2}$ state (the D2 transition). For $\sigma^+$ polarization, the $|1, -1\rangle$ state couples to the $m_F = 0$ states of the F = 0, 1, 2 manifolds of the D2 transition. The sum of the squares of the Clebsch-Gordan coefficients from this transition are $1/6 + 5/24 + 1/24 = 5/12$. Taking in to account the D1 and D2 transitions of $^{87}$Rb, the spin dependent lattice potentials for $\sigma^+$ and $\sigma^-$ polarized light of the $|1, -1\rangle$ state are

$$U_{1,-1}^{+} = \frac{I}{4\epsilon_0\hbar c}\left(\frac{5}{12}D_2^2\Big(\frac{-1}{\Delta_2} + \frac{1}{\Sigma_2}\Big) + \frac{1}{6}D_1^2\Big(\frac{-1}{\Delta_1} + \frac{1}{\Sigma_1}\Big)\right)\cos^2(kz + \phi/2) \quad (3.20)$$

$$U_{1,-1}^{-} = \frac{I}{4\epsilon_0\hbar c}\left(\frac{1}{4}D_2^2\Big(\frac{-1}{\Delta_2} + \frac{1}{\Sigma_2}\Big) + \frac{1}{2}D_1^2\Big(\frac{-1}{\Delta_1} + \frac{1}{\Sigma_1}\Big)\right)\cos^2(kz - \phi/2) \quad (3.21)$$

where $\Delta_{1,2} = \omega_L - \omega_{1,2}$ is the detuning from the D1 and D2 resonant transitions and $\Sigma_{1,2} = \omega_L + \omega_{1,2}$. The dipole moments D1 and D2 are 2.99 $ea_0$ and 4.23 $ea_0$ respectively where $e$ is the magnitude of the charge of an electron and $a_0$ is the Bohr radius. The $|1, 1\rangle$ state has the same coefficients in front of the cosine squared factors,

except that the coefficients are exchanged.

$$U_{1,1}^{+} = \frac{I}{4\epsilon_0 \hbar c}\left(\frac{1}{4}D_2^2\left(\frac{-1}{\Delta_2}+\frac{1}{\Sigma_2}\right)+\frac{1}{2}D_1^2\left(\frac{-1}{\Delta_1}+\frac{1}{\Sigma_1}\right)\right)\cos^2(kz+\phi/2) \tag{3.22}$$

$$U_{1,1}^{-} = \frac{I}{4\epsilon_0 \hbar c}\left(\frac{5}{12}D_2^2\left(\frac{-1}{\Delta_2}+\frac{1}{\Sigma_2}\right)+\frac{1}{6}D_1^2\left(\frac{-1}{\Delta_1}+\frac{1}{\Sigma_1}\right)\right)\cos^2(kz-\phi/2) \tag{3.23}$$

Using Eq. 3.10, it is possible to constrain the lattice depth for a particular species of atoms and solve for the intensity necessary to achieve the lattice depth for a given spin dependent interaction ratio $U_{ab}/U_\sigma$. If maximally stretched hyperfine states are chosen, it greatly simplifies the analysis of the spin dependent potential because both species are guaranteed to have the same lattice depth by symmetry. Secondly, the angle $\beta_a = -\beta_b$ (defined by Eq. 3.12) is $\Delta x = |\beta_{a,b}|/k$. Using this and Eq. 3.16, it is possible to solve for $\phi$ in terms of the spin dependent interaction ratio.

$$\phi = \tan^{-1}\left[\frac{U_0^- + U_0^+}{U_0^- - U_0^+}\left(\frac{2}{\sqrt{N_R}}\ln\left(\frac{U_\sigma}{U_{ab}}\right)\right)^{1/2}\right] \tag{3.24}$$

In the above equation, the lattice depth is measured in lattice recoil units $V_d = N_R E_R$ where $N_R$ is the number of recoil units. Using Eq. 3.24 for $\phi$ and fixing the spin dependent interaction ratio, it is possible to solve for the neccessary laser intensity as a function of wavelength to achieve a certain lattice depth. The plot in Fig. 3.3 shows the required intensity as a function of wavelength for $^{87}$Rb for a fixed pseudo spin interaction ratio of 1/4 and fixed lattice depth of 15 $E_R$. There are several features of note in the plot. For wavelengths near the D1 and D2 lines of Rb, the required power to make a spin dependent optical lattice is very low because one species will interact much more strongly with the optical lattice than the other (at the expense of scattering). Moving farther away from resonance requires more laser intensity for a fixed lattice depth and pseudo spin interaction ratio.

It is tempting to simply tune the laser near an atomic resonance to achieve a deep lattice and a large spin dependent interaction with relatively little laser power. However, the scattering rate greatly increases near resonance. The relevant energy scales for super exchange are $t^2/U \approx 1$Hz for atomic physics experiments, so the scattering

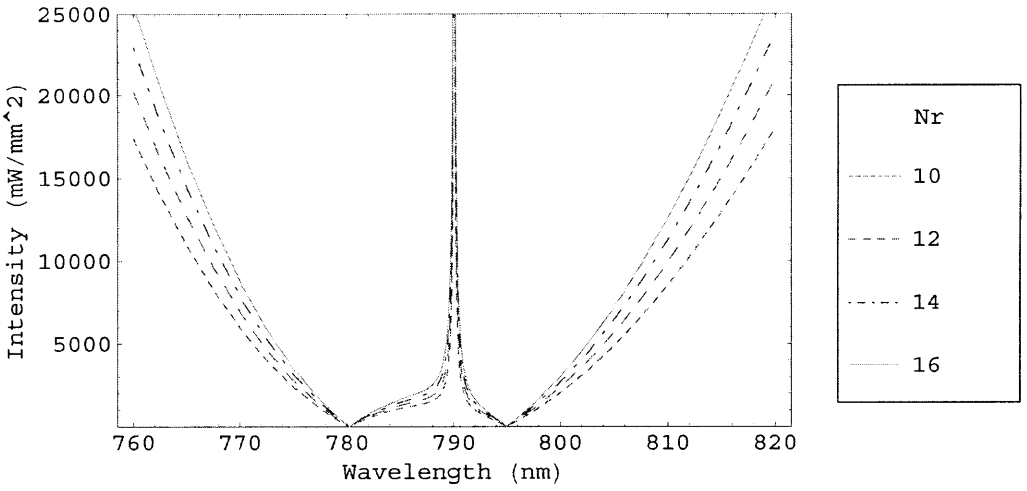


Figure 3-3: Laser intensity required to produce a lattice with $Uab/U_\sigma = 1/4$. This ratio of onsite pseudo spin interaction energies places the system well in to the XY-ferromagnetic regime for equal pseudo-spin species tunneling energies ($\beta = 2$). The required laser intensity for several lattice depths are plotted in units of lattice recoils $N_R$. With rubidium atoms, a lattice depth of $N_R = 15$ has been shown experimentally to be in the Mott-insulating regime. The general trend for blue and re-detuned lattices is that for fixed wavelength and pseudo-spin interaction energy, the laser power increases for deeper lattices as expected. The power requirements for rubidium are not that severe. For example, at $\lambda = 775$ nm, the required laser intensity is approximately 4000 mW/mm2 for lattice depth of 15 recoils and $U_{ab}/U_\sigma = 1/4$. If a laser is focused down to a waist size of 300$\mu$m, the necessary laser power for that laser beam is approximately 280 mW. Tuning the laser wavelength closer to an atomic transition decreases the necessary power, but the scattering rate of the atoms increases significantly.

rate from the lattice light should be low. Experimentally, the laser wavelength should be detuned enough so that the lifetime for scattering ($1/\gamma$) is long compared to any dynamic time scales in the experiment necessary for the atomic system to achieve thermodynamic equilibrium. The time scale should be of order the tunneling time multiplied by the system size. This balance between laser intensity and lifetime is possible because the lattice depth depends linearly on the laser power and as $1/\Delta^2$ while the lifetime varies as $\Delta^2/I$.

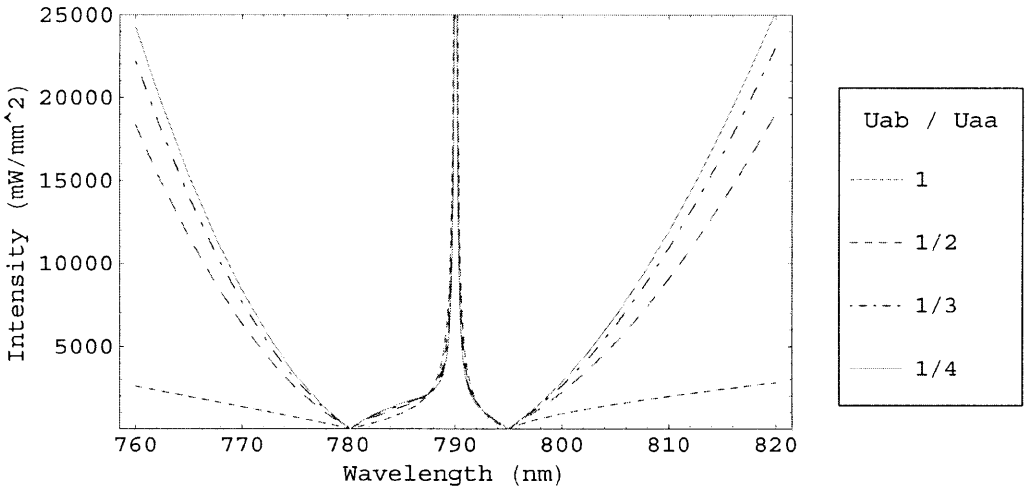


Figure 3-4: Laser intensity required to produce a 15 recoil lattice depth for varying pseudo spin interaction energy ratios $U_{ab}/U_{\sigma}$ as a function of wavelength. Generally, a smaller ratio of $U_{ab}/U_{\sigma}$ requires more laser power. The laser power requirements are less for wavelengths near atomic transitions, but the spontaneous scattering rate increases greatly. The power requirements for sweeping from $U_{ab}/U_{\sigma} = 1$ to $U_{ab}/U_{\sigma} = 1/4$ require a laser intensity sweep from 1000 mW/mm$^2$ to 4000 mW/mm$^2$ for $\lambda =$ 775nm. If the laser beam is focused down to a beam waist of 300 $\mu$m, the laser power sweep is from approximately 70 mW to 280 mW. This laser power sweep will cause the rubidium atoms to undergo a phase transition from a ferromagnetic state to an XY ferromagnetic state as a result of the magnetic super-exchange mechanism.

The time averaged power from an oscillating dipole is given by the Larmor formula

$$P = \frac{\omega^4 d^2}{12\pi\epsilon_0 c^3} \tag{3.25}$$

The classical dipole moment can be replaced with the quantum mechanical version

$$d = \frac{D^2 E}{\hbar^2}\left(\frac{-1}{\Delta} + \frac{1}{\Sigma}\right) \tag{3.26}$$

where $D^2$ is the square of the dipole moment multiplied by the square of the appropriate Clebsch-Gordan coefficient and E is the amplitude of the electric field. The scattering rate is the power scattered divided by the energy per photon scattered, so

the scattering rate is

$$\Gamma = \frac{\omega^3 D^4 I}{6\pi\epsilon_0^2\hbar^3 c^4}\Big(\frac{-1}{\Delta} + \frac{1}{\Sigma}\Big)^2 \tag{3.27}$$

This scattering rate should be summed over all possible $\sigma_+$ and $\sigma^-$ transitions. For example, the scattering rate from the $|1,-1\rangle$ state of $^{87}$Rb is

$$\Gamma^+_{1,-1} = \frac{I\omega^3}{6\pi\epsilon_0^2\hbar^3 c^4}\Big(\frac{7}{96}D_2^4\Big(\frac{-1}{\Delta_2} + \frac{1}{\Sigma_2}\Big)^2 + \frac{1}{72}D_1^2\Big(\frac{-1}{\Delta_1} + \frac{1}{\Sigma_1}\Big)^2\Big)\cos^2(kx + \phi/2) \tag{3.28}$$

$$\Gamma^-_{1,-1} = \frac{I\omega^3}{6\pi\epsilon_0^2\hbar^3 c^4}\Big(\frac{1}{16}D_2^4\Big(\frac{-1}{\Delta_2} + \frac{1}{\Sigma_2}\Big)^2 + \frac{1}{4}D_1^2\Big(\frac{-1}{\Delta_1} + \frac{1}{\Sigma_1}\Big)^2\Big)\cos^2(kx - \phi/2) \tag{3.29}$$

where the cosine squared factors are the result of the spatially varying electric field and the total scattering rate is the sum of $\Gamma^+$ and $\Gamma^-$. The atoms are confined at electric field maxima for red-detuned lattces and electric field minima for blue-detuned lattices. One might expect then that blue detuned lattices always have a lower spontaneous scattering rate than red detuned lattices. However, the atomic wave function is not a delta function- the ground state of wavefunction of ultra cold atoms in an optical lattice in the Mott insulating phase can be approximated as a collection of gaussian wave packets. These wave packets have finite spatial extent, so even in blue detuned optical lattices, the atoms still see an appreciable, non zero electric field. For typical trap fequencies of order 10 kHz, the variance in the atomic position is given by $\sigma = \sqrt{\hbar/m\omega} \approx 100$ nm. If the scattering rate as a function of position above is written as $\Gamma(x) = R^+\cos^2(kx + \phi/2) + R^-\cos^2(kx - \phi/2)$, then the scattering rate is a convolution of atomic probability density with the scattering rate as a function of position $\Gamma(x)$

$$\Gamma_{tot} = \int |w(x - x')|^2\Gamma(z')dx' \tag{3.30}$$

$$= \frac{\Gamma^+}{2}\Big(1 + e^{-1/\sqrt{N_R}}\cos^2(2kx_0 + \phi) + \frac{\Gamma^-}{2}\Big(1 + e^{-1/\sqrt{N_R}}\cos^2(2kx_0 - \phi)\Big) \tag{3.31}$$

with $\sigma^2 = \hbar/2m\omega$ and $x_0$ is the potential energy minimum. Using Eq. 3.11 and Eq. 3.12, the potential minima in the above cosine terms are approximately at $2kx_0 =$

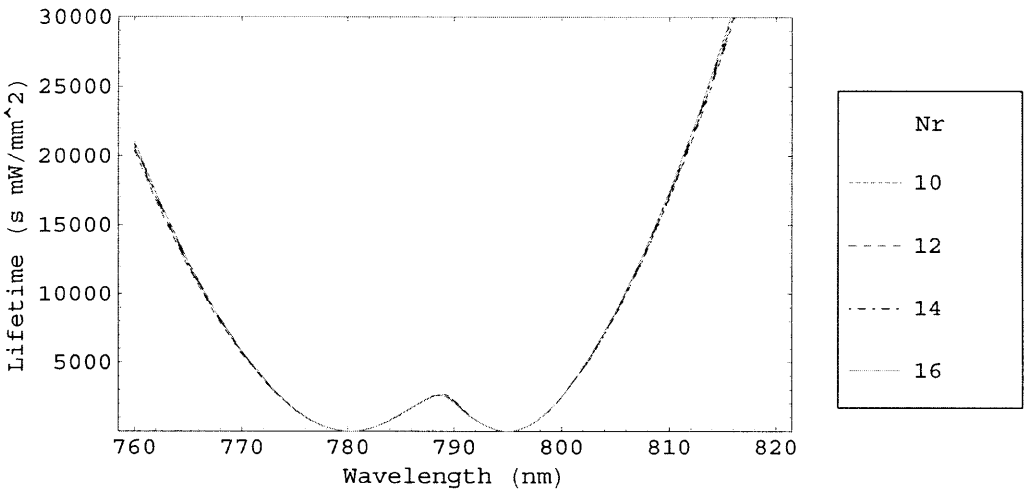


Figure 3-5: Light scattering from an optical lattice versus wavelength for several lattice depths. The y axis is the reciprocal scattering rate (lifetime) multiplied by the intensity of the light and shows the lifetime dependence as a function of lattice wavelength for several lattice depths measured in recoil units. The ratio of the inter species interaction energy to the intra species interaction energy is $U_{ab}/U_\sigma = 1/4$.

$n\pi + \psi$ with

$$\psi = \left[\frac{2}{\sqrt{N_R}} \ln\left(\frac{U_\sigma}{U_{ab}}\right)\right]^{1/2} \tag{3.32}$$

The value n varies depending on the laser detuning, but for $\lambda < 780$nm and $\lambda$ between 790nm and 795 nm, $n \approx 1$. For $\lambda > 795$nm or $\lambda$ between 780nm and 795nm, $n \approx 0$. Each cosine term may then be written as $\cos^2(2kz_0 \pm \phi) = \cos^2(n\pi + \psi \pm \phi)$. Plots of the lifetime $\tau = 1/\Gamma$ per intensity in mW/mm$^2$ are given in Fig. 3.3 as a function of wavelength for several different lattice depth values in recoil units $N_R$.

The above prescription allows one to vary the angle $\phi$ and move the potential minima of two different hyperfine species apart. The separation of the potential minima affects the wavefunction overlap and hence the pseudo-spin interaction energy ratio $U_{ab}/U_\sigma$. Starting with $\phi = 0$ means the lattice minima are not separated, and $U_{ab}/U_\sigma = 1$. This puts the system in a z-ferromagnetic state; all of the spins are aligned. Varying the angle $\phi$ will decrease the pseudo spin interaction ratio, moving the system to the left on the phase diagram in Fig. 2.2. This will be enough to take

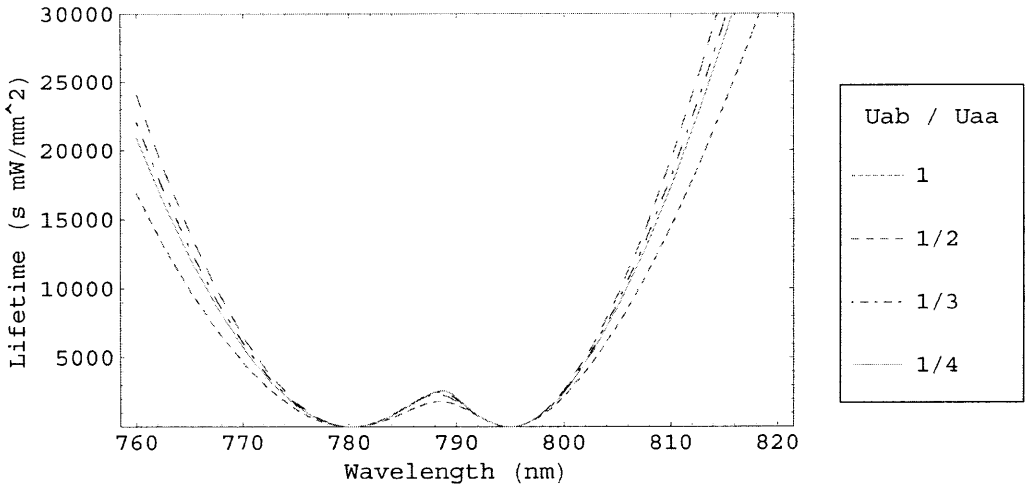


Figure 3-6: Light scattering from an optical lattice versus wavelength for ratios of the inter to intra species interaction energies as a function of lattice wavelength. The lifetime (reciprocal scattering rate) is multiplied by the laser intensity. The lattice depth is fixed at 15 recoils so the system is well in the Mott insulating regime.

the system from a ferromagnetic state to an xy ferromagnetic state. The existence (and subsequent detection) of an xy ferromagnetic state directly tests the theory of magnetic superexchange. The superexchange mechanism is responsible for the phase transition.

## 3.4 Tunneling Asymmetry in Spin Dependent Optical Lattices

In order to get to an antiferromagnetic, z-Neel ordered state, it is necessary to increase the differential tunneling of the two pseudo-spin species. The tunneling of the stretched hyperfine states, such as the $|1, \pm 1\rangle$ state of $^{87}$Rb, are the same, so it is not possible to use the above recipe to achieve antiferromagnetic ordering. There are several ways to make a differential tunneling of the two pseudo-spin hyperfine states. The simplest way is vary the intensity of the $\sigma^+$ and $\sigma_-$ lattices by using elliptically polarized light in the lattice instead of linearly polarized light.

The tunneling asymmetry is given by

$$\beta_t = \frac{t_a}{t_b} + \frac{t_b}{t_a} \tag{3.33}$$

where $t_{a,b}$ is the tunneling term in the Bose Hubbard Hamiltonian. The tunneling asymmetry $\beta_t$ take a constant value of 2 for equal depth lattices for both pseudo-spin species. Each species tunnels between its own optical optical potential minimum, and since both potentials are equally deep for stretched hyperfine states, the tunneling terms must be equal to each other, i.e. $t_a = t_b$. This equality could be broken by choosing atoms in different hyperfine manifolds such as the F = 1 and F = 2 ground state manifolds of $^{87}$Rb, or by simply choosing non stretched states within the same hyperfine manifold ($|1,-1\rangle$ and $|1,0\rangle$). This complicates the above analysis somewhat in the sense that it is not possible to move directly left and right on the phase diagram because the two spin species will not be in equally deep lattices. Experimentally, it is necessary that the two spin species sit in lattices of varying depth to make a differential amenable to realizing antiferromagnetic ordering. By varying the angle $\phi$ and the intensities of the two circular polarizations, it is possible to search the entire phase diagram in Fig. 2.4. The tunneling terms are given by [25]

$$t_\sigma = \frac{4}{\sqrt{\pi}} E_R^{1/4} U_\sigma^{3/4} e^{-2\sqrt{U_\sigma/E_R}} \tag{3.34}$$

Curiously, there seems to be some disagreement over this expression in the literature, even amongst the authors of the above paper. In another paper, the expression for the tunneling is [30]

$$t = \frac{\pi^2}{4} U_\sigma e^{-\pi^2/4\sqrt{U_\sigma/E_R}} \tag{3.35}$$

which does not agree with the author's earlier expression for the tunneling in Eq. 3.34. Attempting to resolve this puzzle by calculating $t_\sigma$ directly according to [28] leads to a third expression for $t_\sigma$.

$$t_{ij} = \int w(x - x_i)\Big(\frac{p^2}{2m} + \frac{1}{2}m\omega^2 x^2\Big) w(x - x_j) dx \tag{3.36}$$

where $t_{ij}$ is the tunneling from lattice site i to lattice site j and $\omega$ is the trap frequency of the periodic optical lattice potential expanded about the potential minima. By replacing the Wannier functions in the above expression with Gaussian wave packets, and by recognizing that a gaussian wave packet is an eigenfunction of the harmonic oscillator Hamiltonian,

$$t_{ij} = \int w(x - x_i)\left(\frac{\omega}{2}\right)w(x - x_j)dx = 3\sqrt{E_R U_\sigma}\, e^{-\frac{\pi^2}{4}\sqrt{\frac{U_\sigma}{E_R}}} \tag{3.37}$$

and disagrees with both [25] and [30]. The common feature is that all depend on the inter species interaction energy to some power multiplied by an exponential with the square root of the inter species interaction energy measured in units of the recoil energy. Therefore, displacing the lattice potential minimum location does not create any tunneling asymmetry. Using maximally stretched hyperfine states results in no tunneling asymmetry because the inter species interaction energies will be the same by symmetry. Creating tunneling asymmetry will require using non maximally stretched hyperfine states, using different hyperfine manifolds (such as the F = 1 and F = 2 hyperfine manifolds in Rb), or using separate circularly polarized lattices with adjustable powers in each polarization.

# Chapter 4

# Seeing Magnetic Super Exchange with Polarization Rotation Imaging

## 4.1 Polarization Rotation Imaging

Polarization rotation imaging is a dispersive imaging technique that relies on an object having different indices of refraction for different polarizations of light. Consider an atomic sample in an applied uniform magnetic field in the z-direction. If incident light along the z-direction is linearly polarized in the x-y plane, the polarization of light can be written as a superposition of $\sigma^+$ and $\sigma^-$ polarizations. These orthogonal polarizations in general couple to different Zeeman sublevels differently, resulting in a differential phase shift of the two circular polarizations. This differential phase shift means that the linear polarization direction is rotated through some angle, and the rotation angle can be measured by the use of a linear polarizer. As will be shown, if the atomic sample is a mixture of two different Zeeman levels, the rotation angle will be linearly proportional to the density difference of the atomic species given certain assumptions about detuning from the Zeeman sublevels.

As a simple model, consider an atomic species in an $F = 1$ state with some population in $m_F = -1$ and the remaining population in $m_F = 1$ state. An applied magnetic field in the z direction breaks the degeneracy of the ground state manifold, and in the small field limit, the Zeeman energy in frequency units is $g_F \mu_B B_z$ where

the Bohr magneton is $\mu_B = 1.4$ MHz/G and $g_F$ is the Lande g-factor. If these atoms are coupled to an $F = 0$ excited state by linearly polarized light in the x-direction, an incident plane wave polarized in the z-direction can be written as a superposition of circularly polarized light

$$E = \hat{x}E_0 e^{i(k_z z - \omega t)} = \frac{E_0}{\sqrt{2}} e^{i(k_z z - \omega t)}(\hat{\sigma}^+ + \hat{\sigma}^-) \tag{4.1}$$

with $\hat{\sigma}^{\pm}$ as the circular polarization unit vectors. In an atomic sample, the k-vector should be multiplied by the index of refraction, and in general the index of refraction has both real and imaginary components. The real part of the index of refraction will cause the wave to accumulate a phase while the imaginary part of the index of refraction leads to absorption by the atomic sample. The real part of the index of refraction is related the the linear susceptibility of the sample by $Re(n) = 1 + Re(\chi)/2$. The real part of the linear susceptibility for $\sigma^{\pm}$-polarized light is [35]

$$Re(\chi_{\pm}) = -\frac{N_{\mp 1}|d|^2}{\epsilon_0 \hbar} \frac{\Delta \mp g_F \mu_B B_z}{(\Delta \mp g_F \mu_B B_z)^2 + \Gamma^2/4 + \Omega^2/2} \tag{4.2}$$

In the above equation, $N_{\mp 1}$ refers to the atomic density of atoms in the $|1, \mp 1\rangle$ state, $d$ is the dipole moment of the transition multiplied by the appropriate Clebsch-Gordan coefficient, $\Gamma$ is the width of the transition, $\Omega = dE_0/\hbar$, and $\Delta$ is the detuning from the F = 0 to F = 1 transition with no magnetic field ($\Delta = \omega_L - \omega_0$). The accumulated phase for an atomic species in the $m_F = \pm 1$ state is given $\Delta\phi = \omega_L \ell / c \cdot \Delta n$ where $\omega_L$ is the laser frequency, $\ell$ is the length of the atomic sample, and $\Delta n$ is the difference in the indices of refraction for $\sigma^+$ and $\sigma^-$ light for each species. The phase delay for each species is

$$\Phi_{\pm 1} = \pm \frac{\omega \ell N_{\pm 1} D_{\pm 1}^2}{2\epsilon_0 \hbar c} \left( \frac{\Delta \pm g_F \mu_B B_z}{(\Delta \pm g_F \mu_B B_z)^2 + \Gamma^2/4 + \Omega^2/2} \right) \tag{4.3}$$

The rotation angle $\theta$ is the difference in the phase delays $\Delta\phi$ divided by two. The factor of two comes from the fact that rotating light that is linearly polarized in the x-direction by 180 degrees results in light that is still polarized in the x-direction.

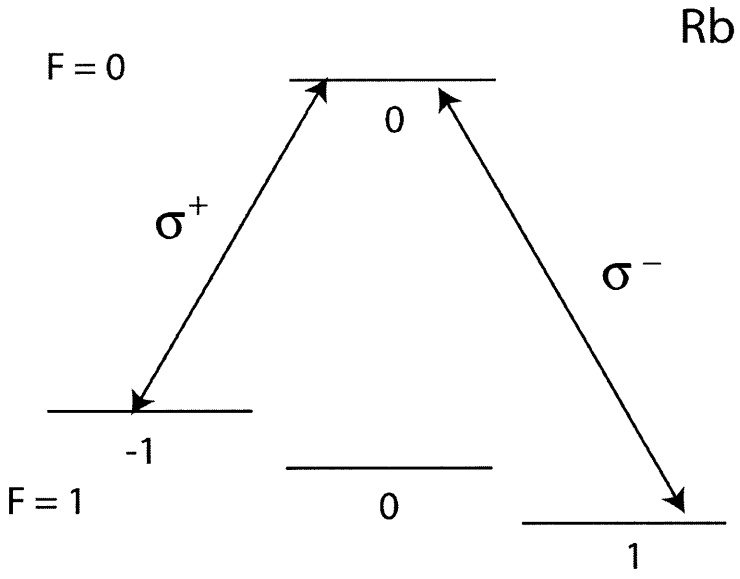


Figure 4-1: Simple model for polarization rotation by coupling an F = 1 manifold to an F = 0 manifold. The detuning $\Delta$ is defined by the energy difference between the $|1,0\rangle$ state and the $|0,0\rangle$ state. In general, the couplings of the hyperfine levels in the ground state manifold to all excited states should be considered.

The rotation angle is therefore

$$\theta = \frac{\omega \ell D^2}{4\epsilon_0 \hbar c}\left(\frac{N_{+1}(\Delta + g_F \mu_B B_z)}{(\Delta + g_F \mu_B B_z)^2 + \Gamma^2/4 + \Omega^2/2} - \frac{N_{-1}(\Delta - g_F \mu_B B_z)}{(\Delta - g_F \mu_B B_z)^2 + \Gamma^2/4 + \Omega^2/2}\right) \quad (4.4)$$

There are several noteable features of the above equation. If the detuning $\Delta$ is zero and the system is only in the $|1,\pm 1\rangle$ hyperfine states (or any other maximally stretched hyperfine state), then the rotated angle is linearly proportional to the sum of the densities. Setting $\Delta = 0$ in the above equation yields:

$$\theta = \frac{\omega \ell D^2}{4\epsilon_0 \hbar c} \frac{g_F \mu_B B_z}{(g_F \mu_B B_z)^2 + \Omega^2/2}(N_{+1} + N_{-1}) \quad (4.5)$$

Note that for fixed atom number $NV$, the polarization rotation angle is independent of fraction of atoms in a particular hyperfine state. In the limit of large detuning compared to the Zeeman energy and $\Omega$, the rotated angle is linearly proportional to

the density difference of the two species $\Delta \gg g_F \mu_B B_z, \Omega$:

$$\theta = \frac{\omega \ell D^2}{4\epsilon_0 \hbar c \Delta}(N_{+1} - N_{-1} + O(\frac{g_F \mu_B B_z}{\Delta})) \tag{4.6}$$

The large detuning limit is particularly interesting because two different hyperfine species rotate the angle of the linear polarization in equal but opposite directions (to order the ratio of the Zeeman energy to detuning). This fact can be used to measure deviations from an equal mixture of spins as a function of space. Consider the following experimental imaging setup. Linearly polarized light is incident on an atomic sample. If the atoms are in an equal mixture of hyperfine levels, there is no net polarization rotation. If this light then impinges on a linear polarizer oriented 45 degrees relative to the initial polarization direction and is imaged on a CCD array, the light intensity will be half of the original light intensity. If the atomic sample has any deviation from an equal mixture, there is a net rotation of the light polarization. The linear polarizer then lets either more or less light through, depending on the concentration of the hyperfine species. In the context of magnetic ordering, Farady rotation imaging is then a direct measure of the magnetization of the sample in the limit of large detuning. Any magnetic domains that form in the sample will either appear lighter or darker than background (zero magnetization).

Faraday rotation imaging is a dispersive imaging technique. Absorption of light by the atomic sample will in general result in less light passing through the imaging system, resulting in an offset in a magnetization measurement. If the absorption is significant and varies appreciably as a function of the magnetization, the measurement of the magnetization can be biased. Increasing the laser detuning eliminates absorption but results in less rotation of the polarization direction for a given deviation from zero magnetization. There is a tradeoff between sensitivity to small amounts of small magnetization (small detuning) and magnetization measurement accuracy (small absorption by large detuning). The amount of absorption can be calculated

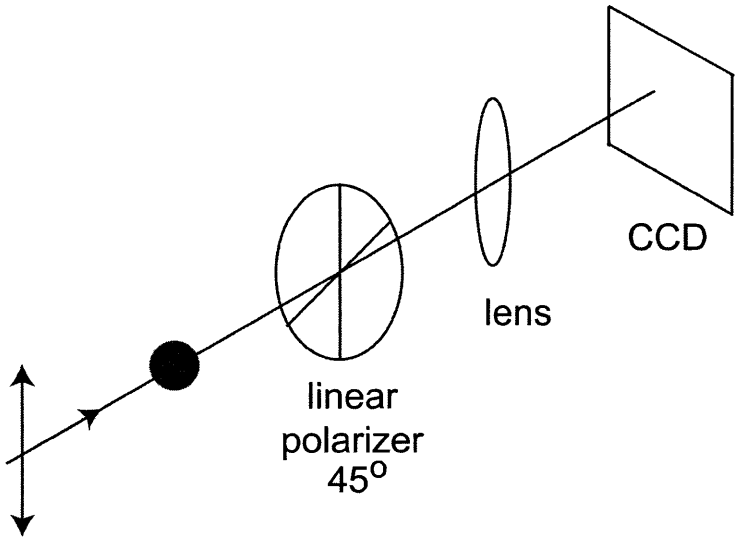


Figure 4-2: Linearly polarized light impinges on an atomic sample in some mixture of hyperfine states. The atoms cause the light to undergo differing phase delays depending on the hyperfine states of the atom, and if the hyperfine states of the atomic sample are maximally stretched (ex: $|F, m_F\rangle = |1, \pm 1\rangle$), the linearly polarized light will be rotated in equal but opposite directions for each hyperfine state. The linear polarizer will let more or less light through depending on the direction of rotation of the linear polarization. A lens images the light on a CCD array, and the resulting image intensity on the CCD array is proportional to the net magnetization of the atomic sample in the limit of large detuning.

from the imaginary part of the index of refraction [35]

$$Im(n_{\pm}) = \frac{Nd^2}{2\epsilon_0 h} \frac{\Gamma/2}{(\Delta \pm g_F \mu_B B_z)^2 + \Gamma^2/4 + \Omega^2/2} \tag{4.7}$$

where $n_{\pm}$ refers to the index of refraction for $\sigma^{\pm}$ polarized light. In the limit of large detuning, the imaginary part of the index of refraction is

$$Im(n_{\pm}) \approx \frac{ND^2\Gamma}{4\epsilon_0 h \Delta^2}(1 \mp O(\frac{g_F \mu_B B_z}{\Delta})) \tag{4.8}$$

The absorption of the $\sigma^{\pm}$ light is $1/2 \cdot exp(-\omega \ell Im(n_{\pm})/c)^2$, so the intensity fraction

of the transmitted light in the limit of large detuning is (correct to order $1/\Delta^2$)

$$\frac{I}{I_0} = 1 - \frac{\omega \ell \Gamma D^2}{2c\epsilon_0 h \Delta^2}(N_+ + N_-) \tag{4.9}$$

In order to directly probe the magnetization of the atomic sample, it is necessary to minimize the absorption of the light by the atomic sample while maintaining a large enough polarization rotation angle to be sensitive to small magnetization changes of the sample. In the large detuning limit, the absorption of light is proportional to $1/\Delta^2$ while the Faraday rotation angle is proportional to $1/\Delta$. The different scaling with detuning allows for such an optimization.

If the detuning is fixed at $\Delta = 0$, then the Farady rotation signal is proportional to the sum of the atomic concentrations $N_+ + N_-$. The imaginary part of the index of refraction in the limit of a large applied magnetic field (compared to the linewidth of the $\sigma^{\pm}$ transitions and $\Omega$) is

$$Im(n_{\pm}) \approx \frac{N_{\pm} D^2 \Gamma}{4\epsilon_0 h (g_F \mu_B B_z)^2} \tag{4.10}$$

The resulting intensity absorption is

$$\frac{I}{I_0} \approx 1 - \frac{\omega \ell \Gamma D^2}{4c\epsilon_0 h (g_F \mu_B B_z)^2}(N_+ + N_-) \tag{4.11}$$

This equation has the same form as the equation for absorption of the atomic sample in the limit of large detuning. The application of a magnetic field pushes the $\sigma^{\pm}$ transitions farther out of resonance, so this result is not surprising. Practically, for alkali atoms like rubidium, increasing the magnetic field to cut down on light absorption requires fairly large magnetic fields ($\approx$ 100 Gauss) to detune the laser a light from resonance by a few linewidths.

For a system like Rb, there are multiple allowed transitions, so the phase delay and subsequent rotation angles should be summed over the allowed dipole transitions. Plots of the rotation angle as a function of $m_F = -1$ fraction are given for various detunings from the $|1,0\rangle \rightarrow |0,0\rangle$ energy at an applied field of 10 Gauss. A plot of the

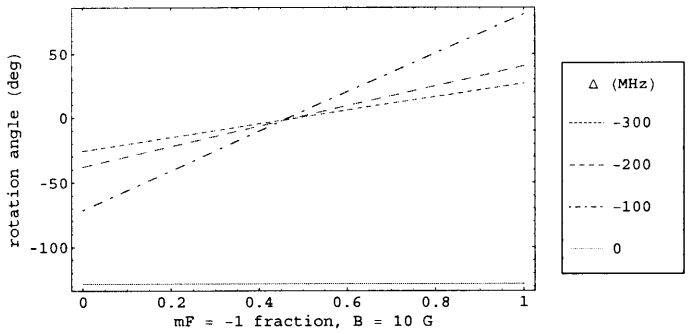


Figure 4-3: Faraday rotation angle as a function of $m_F = -1$ fraction for various detunings at a fixed magnetic field of 10 Gauss. The assumed laser intensity is 10 mW/cm$^2$ incident on a cloud of $10^5$ atoms confined in a spherical volume with a 10 $\mu$m diameter. As can be seen by the plot, at zero detuning (defined as the $|1,0\rangle \rightarrow |0,0\rangle$ energy), the rotation angle is independent of hyperfine species fraction in the cloud. This happens because of symmetry; the $m_F = \pm 1$ levels suffer equal but opposite detunings when an imaging laser is tuned near the transition to the $f = 0$ hyperfine manifold. This causes an equal but opposite phase delay which cancels upon subtracting the phase delays to calculate the Faraday rotation angle.

fraction of the intensity transmitted through the atomic sample is given as a function of $m_F = -1$ fraction for various detunings at a field of 10 Gauss.

Since Faraday rotation imaging is directly proportional to the magnetization of an atomic cloud, it may be well suited for measuring a cold atomic cloud with magnetic ordering that varies as a function of space. The setup in Fig. 4.1 should allow more light to reach the CCD camera as one atomic species rotates the light polarization toward the linear polarizer's polarizing axis. The other hyperfine species will rotate the polarized light farther from the linear polarizer's polarization axis, resulting in less light reaching the CCD camera. In a non-spin dependent lattice, the effective Heisenberg Hamiltonian should make bosonic atoms in a lattice align ferromagnetically, with possible domain structure being driven by ambient uncontrolled magnetic field gradients. The resulting dispersive image from the proposed Faraday rotation imaging scheme should show domains as black and white spots. This offers an opportunity to directly observe the super exchange mechanism as well as any time dependence of domain growth.

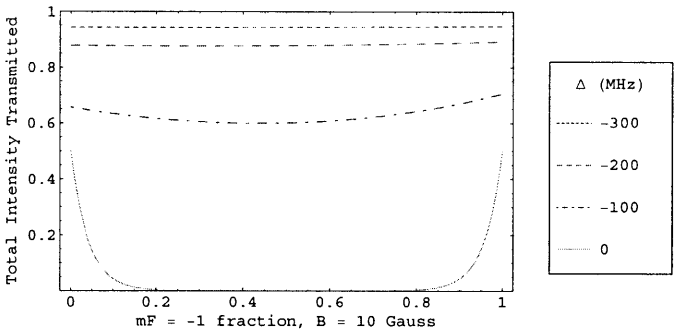


Figure 4-4: Transmission intensity fraction as a function of $m_F = -1$ fraction for various detunings at a fixed magnetic field of 10 Gauss. The assumed laser intensity is 10 mW/cm$^2$ incident on a cloud of $10^5$ atoms confined in a spherical volume with a 10 $\mu$m diameter. Detuning away from the $F = 0$ energy decreases the total absorption of the could and will not bias the results of reading out the magnetization of the cloud as the hyperfine concentration varies across the cloud at the expense of sensitivity to deviations from zero magnetization.

To drive the system to order as an XY ferromagnet, it is possible to create a spin dependent lattice by experimentally controlling an electro-optic modulator as described in the previous chapter. As the spin dependence of the lattice is increased (a decrease in the ratio of the inter to intra species interaction energies $U_{ab}/U_\sigma$), the ferromagnetic ordering should change to XY ferromagnetic ordering. The amount of magnetization in the z-direction should decrease, and deep in the XY regime, the atomic cloud will appear indistinguishable from the background as the magnetization in the z-direction decreases.

It is also possible to control the size of an XY domain by applying a magnetic field gradient across the could. If there is no spin dependence in the lattice, a large field gradient will cause the atoms to form one domain wall in the center of the cloud. If the spin dependence of the lattice is turned on and the magnetic field gradient is lowered, an XY ferromagnetic domain will form in the center of the cloud. As the field gradient is lowered, the XY domain should grow to the system size. It is possible to get an estimate on the field gradients needed by performing a variational calculation. Using the following wave function, it is possible to minimize the energy with respect

to the angle $\theta$ which measures the spin polarization out the XY plane:

$$H = \sum_{\langle ij \rangle} \lambda_z \sigma_i^z \sigma_j^z - \lambda_\perp (\sigma_i^x \sigma_j^x + \sigma_i^y \sigma_j^y) - \sum_i h_z \sigma_i^z \tag{4.12}$$

$$\psi = \cos(\theta)\overrightarrow{x} + \sin(\theta)\overrightarrow{y} \tag{4.13}$$

Minimizing this energy with respect to $\theta$ gives the canting angle and is shown in Fig. 4.1:

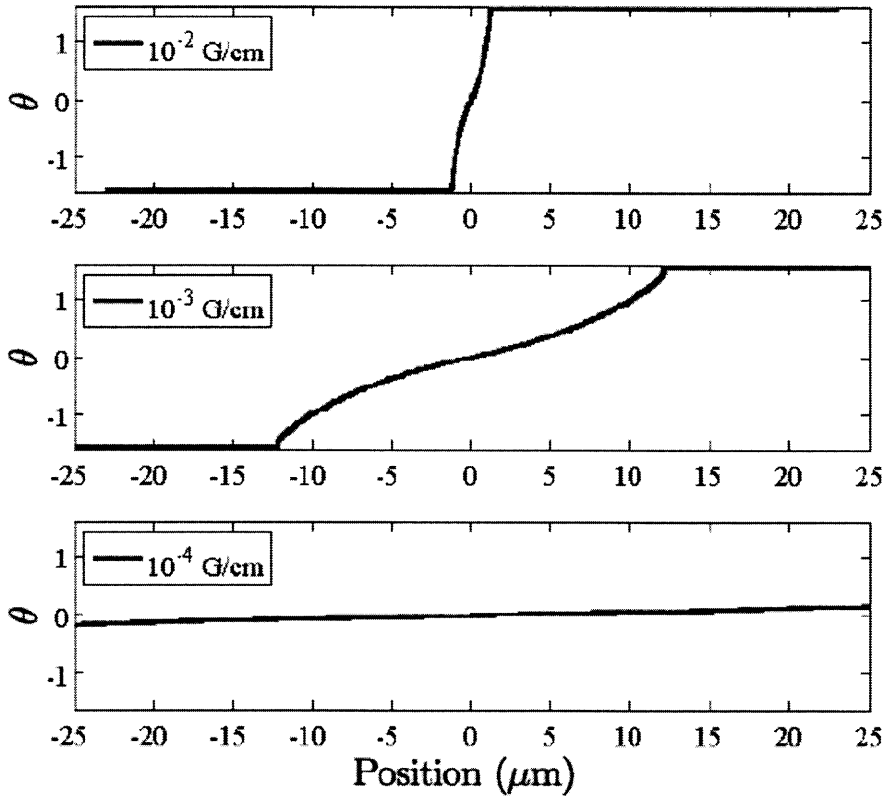


Figure 4-5: Canting angle out of the XY plane versus trap position for various magnetic field gradients. The atomic cloud is 50 $\mu$m in size and is in a lattice with depth 15 $E_R$. The ratio of the inter to intra species interaction energies is $U_{ab}/U_\sigma = 0.8$ and there is no tunneling asymmetry. Decreasing the magnetic field gradient allows an XY ferromagnetic domain to grow in size, until at the 100 $\mu$G/cm level where the XY domain size reaches reaches the approximate system size. These plots also set limits on the tolerable ambient magnetic field gradients; large field gradients will make any XY domains that form very small and the ordering will be driven by the field gradients across the cloud.

# Chapter 5

# Future Prospects and challenges

Confining ultra cold atoms to an optical lattice may proven a useful avenue for investigating condensed matter phenomena such as quantum magnetism and may shed light on the mechanism behind high temperature superconductivity. When bosons are confined to an optical lattice, they behave according the Bose Hubbard model, and in the limit of deep confinement, are modeled by an effective Heisenberg spin Hamiltonian. The Heisenberg spin Hamiltonian predicts the system will order into a wide variety of magnetic phases as a result of the magnetic super exchange mechanism.

Exploring the magnetic ordering phase diagram of this effective Hamiltonian may provide key insights in to the formation of magnetic domains governed by super exchange as well as the opportunity to study domain formation dynamics. It may be possible to see magnetic super exchange by waiting for a two component insulating system to order in a lattice. This form of Z ferromagnetism is driven by magnetic super exchange and competes energetically with local ambient magnetic field gradient fluctuations. It seems possible to observe ordering given the exchange energy, size of the cloud, and expected field gradient fluctuations. The formation of magnetic domains may even be driven by field gradients.

Realizing phases beyond z-ferromagnetism requires the creation of a spin dependent lattice where the inter species interaction energy can be tuned relative to the intra species interaction energy. Tuning this ratio drives the system in to an XY ferromagnetic state. Reaching the antiferromagnetic regime requires decreasing this

interaction energy ratio further and creating a lattice with tunneling energy asymmetry between the two hyperfine species. Such a configuration may be possible by creating elliptically polarized lattices.

Detecting these magnetic phases provides its own set of challenges. One way to see z-ferromagnetism is to use a dispersive imaging technique such as Faraday rotation imaging. Given assumptions about detuning, Faraday rotation imaging directly measures the magnetization of the cold atomic cloud by measuring the density difference of the two hyperfine atomic states. If the system develops finite magnetization in the quantization direction in form of domains, Faraday rotation imaging should be able to directly image these domains, providing the opportunity to observe the ordering and its associated dyanmics.

By driving the system to adopt XY ferromagnetic ordering, the Faraday rotation signal should disappear because the atomic cloud loses its magnetization in the z-direction. It should be possible to observe this transition and investigate its associated dynamics by using an eletro-optic modulator to create spin dependent lattices as described in this thesis.

Observing antiferromagnetic ordering is not possible with Faraday rotation imaging because the system has no macroscopic net magnetization in the z-direction. Antiferromagnetic ordering will produce the same Faraday rotation signal as an XY ferromagnet. There are a few ways to see antiferromagnetic ordering. For example, M. Greiner et al have proposed building a quantum gas microscope capable of resolving individual lattice sites. Taking absorption pictures using this device will show a checkerboard arrangement of hyperfine species in a square lattice. Another way to possibly observe antiferromagnetic ordering is through the use of Bragg scattering off lattice planes. By using a hyperfine state selective laser, it may be possible to observe the suppression and sudden appearance of new Bragg peaks as the period of the lattice doubles when the system goes from ferromagnetic ordering to antiferromagnetic ordering. This seems possible for Rb in a lattice with lattice constant 532 nm and using a laser tuned near either a D1 or D2 transition incident on the (111) plane of the crystal.

There are several remaining challenges to be met before exploring the full Heisenberg Hamiltonian. Because the super exchange energy is so low (of order 1 Hz), cooling the atoms to sufficiently low temperatures is challenging. It may be possible to move entropy out of the system by constructing an analog to adiabatic demagnetization refrigeration. For example, by spatially separating a mixture of hyperfine states in a magnetic field gradient and then slowly lowering the gradient field, it may be possible to move the entropy of the system in to the spin degrees of freedom at the interface of the spin up and spin down sections of the cold atomic cloud. By using optical pumping, it may be possible to move this spin entropy out of the system in the form of photons. It remains to be seen if such a scheme or any other scheme can achieve temperatures low enough for the super exchange mechansim to drive magnetic ordering.

# Bibliography

[1] M.W. Zwierlein, J.R. Abo-Shaeer, A. Schirotzek, C.H. Schunck, and W. Ketterle. Vortices and superfluidity in a strongly interacting fermi gas. *Nature*, 435(1047), 2005.

[2] M.W. Zwierlein, C.A. Stan, C.H. Schunck, S.M.F. Raupach, A.J. Kerman, and W. Ketterle. Condensation of pairs of fermionic atoms near a feshbach resonance. *Phys. Rev. Lett.*, 92(120403), 2004.

[3] M.W. Zwierlein, A. Schirotzek, C.H. Schunck, and W. Ketterle. Superfluidity with imbalanced spin populations. *Science*, 311, 2006.

[4] Y. Shin, M.W. Zwierlein, C.H. Schunck, A. Schirotzek, and W. Ketterle. Observation of a phase separation in a strongly interacting imbalanced fermi gas. *Phys. Rev. Lett.*, 97(030401), 2006.

[5] M.W. Zwierlein, C.H. Schunck, A. Schirotzek, and W. Ketterle. Direct observation of the superfluid phase transition in ultracold fermi gases. *Nature*, 442(54), 2006.

[6] M. Greiner, O. Mandel, T. Esslinger, T.W. Hansch, and I. Bloch. Quantum phase transition from a superfluid to a mott insulator in a gas of ultra cold atoms. *Nature*, 415(39), 2002.

[7] M. Greiner, O. Mandel, T.W. Hansch, and I. Bloch. Collapse and revival of the matter wave field of a bose-einstein condensate. *Nature*, 419(51), 2002.

[8] G.K. Campbell, J. Mun, M. Boyd, P. Medley, A.E. Leanhardt, L. Marcassa, D.E. Pritchard, and W. Ketterle. Imaging the mott insulator shells using atomic clock shifts. *Science*, 313(649), 2006.

[9] S. Foelling, A. Widera, T. Mueller, F. Gerbier, and I. Bloch. Formation of spatial shell structures in the superfluid to mott insulator transition. *Phys. Rev. Lett.*, 97(060403), 2006.

[10] R.P. Feynman. Simulating physics with computers. *International Journal of Theoretical Physics*, 21(467), 1982.

[11] J.J. Garcia-Ripoll and J.I. Cirac. Spin dynamics for bosons in an optical lattice. *New Journal of Phys.*, 5(76.1), 2003.

[12] R.P. Feynman, R.B. Leighton, and M. Sands. *The Feynman Lectures on Physics*, volume 2. Addison-Wesley Publishing Company, 2nd edition, 1964.

[13] A. Auerbach. *Interacting Electrons and Quantum Magnetism.* Springer-Verlag, 1994.

[14] E. Demler, W. Hanke, and S.-C. Zhang. So(5) theory of antiferromagnetism and superconductivity. *Rev. Mod. Phys.*, 76(909), 2004.

[15] S. Sachdev. Order and quantum phase transitions in the cuprate superconductors. *Rev. Mod. Phys.*, 75(913), 2002.

[16] G. Kotliar and D. Vollhardt. Strongly correlated electron materials: insights from dynamical mean-field theory. *Physics Today*, 57(53), 2004.

[17] P.W. Anderson. The resonating valence bond state in la2cuo4 and superconductivity. *Science*, 235(1196), 1987.

[18] T. Senthil and P.A. Lee. Cuprates as doped u(1) spin liquids. *Phys. Rev. B*, 71(174515), 2005.

[19] J. Orenstein and A.J. Mills. Advances in the physics of high-temperature superconductivity. *Science*, 288(468), 2000.

[20] I. Affleck and J.B. Marston. Large-n limit of the heisenberg-hubbard model: Implications for high-tc superconductors. *Phys. Rev. B*, 37(3774), 1988.

[21] W.-G. Wen and P.A. Lee. Advances in the physics of high-temperature superconductivity. *Phys. Rev. Lett.*, 76(503), 1996.

[22] D.H. Kim and P.A. Lee. Theory of underdoped cuprates. *Ann. Phys. (N.Y.)*, 272(130), 1999.

[23] W. Rantner and W.-G. Wen. Spin correlations in the algebraic spin liquid: Implications for high-tc superconductors. *Phys. Rev. B*, 66(144501), 2002.

[24] M. Hermele, T. Senthil, M.P.A Fisher, P.A. Lee, N. Nagaosa, and X-.G. Wen. *Phys. Rev. B*, 70(214437), 2004.

[25] L.-M. Duan, E. Demler, and M.D. Lukin. Controlling spin exchange interactions of ultracold atoms in optical lattices. *Phys. Rev. Lett.*, 91:9, 2003.

[26] D. Jaksch, C. Bruder, J.I Cirac, C.W. Gardiner, and P. Zoller. Cold bosonic atoms in optical lattices. *Phys. Rev. Lett.*, 81(3108), 1998.

[27] M.P.A Fisher, P.B. Weichman, G. Grinstein, and D.S. Fisher. Boson localization and the superfluid-insulator transition. *Phys. Rev. B*, 40(546), 1989.

[28] D. Jaksch and P. Zoller. The cold atom hubbard toolbox. *Annals of Phys.*, 315(52), 2004.

[29] I. Bloch, J. Dalibard, and W. Zwerger. Many-body physics with ultra cold gases. *Rev. Mod. Phys.*, 80(885), 2008.

[30] E. Altman, W. Hofstetter, E. Demler, and M.D. Lukin. Phase diagram of two component bosons on an optical lattice. *New Journal of Physics*, 5:113.1–113.19, 2003.

[31] A.B. Kuklov and B.V. Svistunov. Counterflow superfluidity of two-species ultra cold atoms in a commensurate optical lattice. *Phys. Rev. Lett.*, 90(10), 2003.

[32] M.E. Fisher and D.R. Nelson. Spin flops, supersolids, and bicritical and tetracritical points. *Phys. Rev. Lett.*, 32(1350), 1974.

[33] M.A. Nielsen and I. Chuang. *Quantum Computation and Quantum Information.* Number 192-202. Cambridge University Press, 2002.

[34] O. Mandel, M. Greiner, A. Widera, T. Rom, T.W. Hansch, and I. Bloch. Coherent transport of neutral atoms in spin dependent optical lattice potentials. *Phys. Rev. Lett.*, 91(1), 2003.

[35] C. Cohen-Tannoudji, J. Dupont-Roc, and G. Grynberg. *Atom-Photon Interactions: Basic Processes and Applications.* Wiley-VCH, 1998.